BIOCHEMISTRY
including biophysical chemistry & molecular biology

Article

pubs.acs.org/biochemistry

Nitrite Reductase Activity of Rat and Human Xanthine Oxidase, Xanthine Dehydrogenase, and Aldehyde Oxidase: Evaluation of Their Contribution to NO Formation *in Vivo*

Luisa B. Maia,*[,†] Vânia Pereira,[‡] Lurdes Mira,[‡] and José J. G. Moura*[,†]

[†]UCIBIO, REQUIMTE, Departamento de Química, Faculdade de Ciências e Tecnologia, Universidade Nova de Lisboa, 2829-516 Caparica, Portugal

[‡]CQB, Departamento de Química e Bioquímica, Faculdade de Ciências, Universidade de Lisboa, Campo Grande, 1749-016 Lisboa, Portugal

Supporting Information

ABSTRACT: Nitrite is presently considered a NO "storage form" that can be made available, through its one-electron reduction, to maintain NO formation under hypoxia/anoxia. The molybdoenzymes xanthine oxidase/dehydrogenase (XO/XD) and aldehyde oxidase (AO) are two of the most promising mammalian nitrite reductases, and in this work, we characterized NO formation by rat and human XO/XD and AO. This is the first characterization of human enzymes, and our results support the employment of rat liver enzymes as suitable models of the human counterparts. A comprehensive kinetic characterization of the effect of pH on XO and AO-catalyzed nitrite reduction showed that the enzyme's specificity constant for nitrite increase 8-fold, while the $K_m^{NO_2^-}$ decrease 6-fold, when the pH decreases from 7.4 to 6.3. These results demonstrate that the ability of XO/AO to trigger NO formation would be greatly enhanced under the acidic conditions characteristic of ischemia. The dioxygen inhibition was quantified, and the $K_i^{O_2}$ values found (24.3−48.8 μM) suggest that *in vivo* NO formation would be fine-tuned by dioxygen availability. The potential *in vivo* relative physiological relevance of XO/XD/AO-dependent pathways of NO formation was evaluated using HepG2 and HMEC cell lines subjected to hypoxia. NO formation by the cells was found to be pH-, nitrite-, and dioxygen-dependent, and the relative contribution of XO/XD plus AO was found to be as high as 50%. Collectively, our results supported the possibility that XO/XD and AO can contribute to NO generation under hypoxia inside a living human cell. Furthermore, the molecular mechanism of XO/AO-catalyzed nitrite reduction was revised.

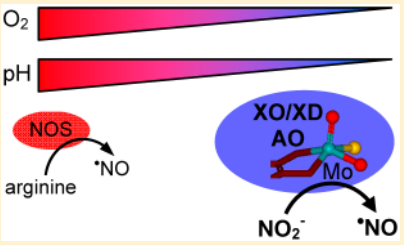

In humans, nitric oxide radical (NO) is involved in several physiological processes, including vasodilation (through the well-known activation of guanylate cyclase), neurotransmission, immune response, platelet aggregation, apoptosis, gene expression, and mediation of antimicrobial activities.[1] Nevertheless, its overproduction (and that of other reactive nitrogen species, in particular peroxynitrite) has been implicated in several pathological conditions, such as chronic inflammation, septic shock syndrome, diabetes, and Parkinson's and Alzheimer's diseases.[2]

Three tissue-dependent isoforms of NO synthase (NOS) (neuronal, endothelial, and inducible) catalyze the formation of NO from dioxygen and the guanidinium nitrogen atom of L-arginine, in a reaction that depends on NADPH.[3−5] The NO biological effects are accomplished, mainly, by posttranslational modification of transition metal centers and of cysteine residues and other thiols, to form nitrosyl (metal−N═O) and *S*-nitrosothiol (R−S−N═O) species, respectively.[2,6−9] To control the specificity of NO signaling and to limit NO toxicity, the NOS activity is tightly regulated and the NO lifetime is controlled through its rapid oxidation to nitrite (e.g., by dioxygen[10,11] or ceruloplasmin[12]) and nitrate (e.g., by oxy-hemoglobin or oxy-myoglobin[1,13−16]).

In addition to the well-known dioxygen-dependent NOS-catalyzed NO formation, it is at present clear that nitrite can also contribute to NO generation, through its one-electron reduction (eq 1), and exert a significant protective action *in vivo*.[17−35] Accordingly, nitrite is being considered a NO "storage form" that can be made available to maintain NO formation under conditions of hypoxia/anoxia, when the oxygen-dependent NOS activity is impaired.[36]

$$NO_2^- + 1e^- + 2H^+ \rightarrow {}^{\bullet}NO + H_2O \quad (1)$$

Although no "dedicated" nitrite reductase was ever found in mammals, numerous metalloproteins, present in cells to conduct other functions, were shown to be able to reduce nitrite to NO: (i) the molybdenum-containing enzymes xanthine oxidase/xanthine dehydrogenase (XO/XD),[37−43] aldehyde oxidase (AO),[42,44] sulfite oxidase,[45] and mitochondrial amidoxime reducing component,[46] (ii) a growing number of heme-containing proteins, where hemoglobin and myoglobin[17,24,31,47,48] stand out in number of publications, but including also neuroglobin,[49]

Received: August 7, 2014
Revised: December 22, 2014
Published: December 23, 2014

DOI: 10.1021/bi500987w
Biochemistry 2015, 54, 685−710

Scheme 1. Mechanism of Nitrite Reduction to NO Catalyzed by XO and AO[a]

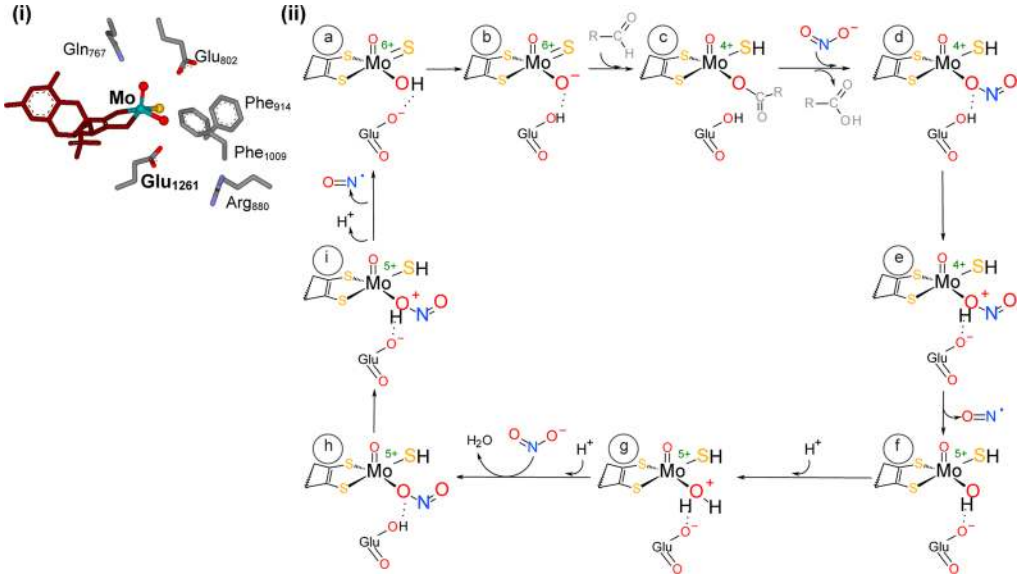

[a](i) Three-dimensional structure of the BMXO molybdenum catalytic center (pyranopterin cofactor colored dark red). (ii) Mechanism of nitrite reduction to NO (see the text for details). The structure shown is based on Protein Data Bank entry 1FO4;[76] the images were produced with Accelrys DS Visualizer (Accelrys Software Inc.).

cytoglobin,[50] cytochrome *c*,[51] and cytochrome P_{450},[52,53] and (iii) several other proteins.[54−57] The nitrite "recycling" to NO is, however, a complex subject, overshadowed by the following main biochemical constraints.[33,34] (i) In the case of the hemic proteins, how can the formed NO avoid being rapidly trapped by the heme itself? (ii) In the case of enzymes, how can nitrite compete with the "classic" oxidizing substrates? (iii) How can we reconcile the *in vivo* observed nitrite effects with the *in vitro* knowledge of nitrite reduction through those diverse pathways?

The *in vitro* and *in vivo* characterization of nitrite reductase pathways is, therefore, of great interest for human physiology and pathology. The *in vitro* characterization allows the kinetic and molecular mechanistic characterization, the quantification of inhibitors and pH effects, and the study of possible regulatory mechanisms of each individual pathway. The *in vivo* studies provide information about the relative physiological relevance of each pathway and how that myriad of pathways can be or are articulated and regulated in a living cell.

In this work, we extended our previous characterization of the nitrite reductase activity of mammalian XO[43] and included also the mammalian AO. Mammalian XO (EC 1.17.3.2) and AO (EC 1.2.3.1) are complex homodimers (290 kDa), belonging to the XO family of molybdoenzymes, that hold one identical molybdenum center (Scheme 1, i), two [2Fe-2S] centers, and one FAD.[58−64] Both enzymes are found in the cytoplasm of various tissues.[65−68] It is noteworthy that XO was described as also being present on the outer surface of the cell membrane of endothelial and epithelial cells[69−73] and of erythrocytes.[25,30] *In vivo*, AO exists exclusively as an oxidase (reduces dioxygen, not NAD^+),[74,75] whereas XO exists predominantly as a NAD^+-dependent dehydrogenase, named xanthine dehydrogenase (XD).[58−64] However, the XD form can be rapidly converted into a strict oxidase form, the XO, that reduces only dioxygen (and not NAD^+); the conversion can be either reversible, through oxidation of Cys_{535} and Cys_{992}, or irreversible, by limited proteolysis at Lys_{551} or Lys_{569} (bovine milk enzyme numbering).[62,76,77] Accordingly, it has been suggested that, while XD is the predominant intracellular form, XO predominates extracellularly, because of the action of plasma proteases.[72,78]

Physiologically, mammalian XO/XD is a key enzyme in purine catabolism, where it catalyzes the hydroxylation of both hypoxanthine and xanthine to the terminal metabolite, urate, with the simultaneous reduction of NAD^+ to NADH (XD) or dioxygen to hydrogen peroxide and superoxide radical anion (both XO and XD).[58−64] The physiological function of AO remains a matter of discussion, being a probable partner in the metabolism of xenobiotics, neurotransmitters, and retinoic acid.[75,79−81] However, XO/XD, as well as AO, also catalyzes the oxidation of a wide variety of substituted pyridines, purines, pteridines, and related compounds, including NADH[82−87] and aldehydes.[58−64,88,89] Besides this broad specificity for reducing substrates, these enzymes are also promiscuous with the oxidizing substrates, being able to catalyze the reduction of several sulfoxides and *N*-oxides, including nitrate and nitrite.[37−44,90] The ability of the enzymes to catalyze the reduction of dioxygen has suggested their involvement in hydrogen peroxide-mediated signaling pathways[91,92] and, most important, in some reactive oxygen species (ROS)-mediated diseases,[93−96] including ischemia-reperfusion injury[97−100] and ethanol hepatotoxicity.[84,101−104] In addition, XO/XD is also the target of development of new drugs against hyperuricemia and gout. The proposed roles of both XO/XD and AO under a range of physiological and pathological conditions have resulted in a considerable and growing medical interest in these enzymes. More recently, the demonstration that XO/XD and AO can also catalyze the nitrite reduction with NO formation contributed to further stimulate interest in the catalytic properties of these versatile enzymes. Remarkably, it also changed the way in which these enzymes are being considered: from damaging (ROS sources) to beneficial players (NO sources) of human metabolism.

To contribute to the characterization of XO/XD- and AO-dependent pathways of NO generation, we studied the activity of rat liver enzymes nitrite reductase/NO synthase as

DOI: 10.1021/bi500987w
Biochemistry 2015, 54, 685−710

models of the human pathways. With this aim, we purified rat liver XO, XD, and AO (RLXO, RLXD, and RLAO, respectively) and fully characterized the kinetics of NO formation at pH 7.4 and 6.3, determined the pH profile of the specificity of the enzymes for nitrite, and quantified the dioxygen inhibition of NO formation and dioxygen-mediated NO consumption (reactions of NO with dioxygen and superoxide radical anion). Simultaneously, we also purified the human liver XO and AO (HLXO and HLAO, respectively) and characterized their nitrite reductase/NO synthase activity. As far as we know, this is the first characterization of the XD form and, most important, of true human enzyme nitrite reductase activity. Our results support the adequacy of rat liver enzymes as models of the human counterparts and demonstrate that it is feasible and reasonable that XO/XD and AO could contribute to *in vivo* NO generation under hypoxic and normoxic conditions.

To evaluate the potential *in vivo* relative physiological relevance of XO/XD- and AO-dependent pathways of NO formation, we used two cell lines, human epithelial cells from liver carcinoma (HepG2) and human microvascular endothelial cells (HMEC), subjected to hypoxia, 23 and 43 μM dioxygen, to mimic the conditions characteristic of ischemia. The NO formation by those cells was followed with a cell-permeable fluorescence probe, and the contribution of XO/XD and AO was evaluated with the use of specific inhibitors (allopurinol, raloxifene, and L-NAME, which are inhibitors of XO/XD, AO, and NOS, respectively). To the best of our knowledge, this is the first study in which cell lines were used to estimate the potential NO formation *in vivo*, and this approach supported the idea that XO/XD and AO can, in fact, contribute to NO generation under hypoxia and even quasi-normoxia.

EXPERIMENTAL PROCEDURES

Materials. All the reagents were of the highest quality available and were used as supplied. Allopurinol, bovine milk XO (BMXO), 4-amino-5-(methylamino)-2′,7′-difluorescein (DAF-FM), DAF-FM diacetate (DAF-FM DA), diethylamine NONOate diethylammonium salt (DEA NONOate), dihydroxybenzaldehyde (DHB), *p*-dimethylaminocinnamaldehyde (DMAC), diphenyleneiodonium chloride (DPI), dithiothreitol, epidermal growth factor (EGF), L-glutamine, hemoglobin, hydrocortisone, mineral oil, NAD^+, NADH, N^{ω}-nitro-L-arginine methyl ester hydrochloride (L-NAME), *N*-methyl-D-glucamine dithiocarbamate (MGD), *N*′-methyl-nicotinamide (NMN), sodium dithionite, sodium nitrite, superoxide dismutase (SOD), raloxifene, rotenone, RPMI-1640 medium (without sodium hydrogen carbonate and phenol red), and xanthine were obtained from Sigma. Fetal bovine serum (FBS), penicillin, streptomicin, and trypsin were obtained from Lonza (Basel, Switzerland). MCDB 131 medium (without glutamine) and MitoXpress (Lux-MX-400-1) were obtained from Gibco (Grand Island, NY) and Luxcel Biosciences (Cork, Ireland), respectively. All the other reagents were from Merck (Darmstadt, Germany).

Enzyme Purification. RLXO and RLAO[a] were purified from adult male Sprague-Dawley rats (3−4 months old) as described previously by Maia and Mira.[108] RLXD was obtained through reversible reduction of oxidized XO sulfhydryl groups. Purified XO was incubated with 5 mM DTT, for 1−2 h at 30 °C, and then passed through a small G-25 column equilibrated in 100 mM Tris-HCl buffer (pH 7.8); a conversion of 85−80% was routinely obtained.[108] HLXO and HLAO were purified in a manner similar to that of the rat liver enzymes. The enzyme concentration was corrected for the presence of inactive molecules assuming that 100% functional XO and AO would have activity-to-flavin ratio (AFR) values of 200[109] and 100,[110] respectively. Except where otherwise specified, the samples of RLXO, RLAO, HLXO, and HLAO used had averaged AFR values of 141, 67.2, 104, and 41.9, respectively. The deflavo forms of RLXO and RLAO (deflavo-RLXO and deflavo-RLAO) were prepared as described by Branzoli and Massey.[111]

NO Measurements by Spin-Trapping and EPR Spectroscopy. The reaction mixtures were prepared in an anaerobic chamber (MBraun UniLab), and all the solutions were first deoxygenated (argon-purged). The ferrous complex of *N*-methyl-D-glucamine dithiocarbamate [$(MGD)_2$-Fe] was prepared by mixing ferrous ammonium sulfate and *N*-methyl-D-glucamine dithiocarbamate to final concentrations of 12.0 and 60.0 mM, respectively. The assays were conducted at 25 °C, in 50 mM phosphate (0.1 mM EDTA) buffer (pH 7.4) containing 10.0−2.00 mM $(MGD)_2$-Fe and other reactants as indicated in the figure legend; the reactions were initiated by adding the enzyme. The reaction mixtures were then transferred to a quartz flat cell and sealed, and the X-band (9.65 GHz) EPR spectra were recorded (at 20 °C) in a Bruker EMX 6/1 spectrometer, with an ER 4102ST cavity (Bruker). The acquisition conditions were as follows: modulation frequency of 100 kHz, modulation amplitude of 0.1 mT, and microwave power of 20 mW.

NO Electrochemical Measurements. Electrochemical measurements of NO were taken with an NO-selective Clark-type electrode (ISO-NO Mark II, World Precision Instruments Inc.). The electrode was calibrated daily with known concentrations of NO, generated with acidified nitrite solutions in the presence of potassium iodide, as described by the electrode manufacturer. The assays were conducted in a 1 mL (final volume) anaerobic cell (World Precision Instruments Inc.), at 25 °C, in 50 mM phosphate (0.1 mM EDTA) buffer (pH 7.4) [except for the study of pH and dioxygen effects (see below)], and all the solutions were first deoxygenated (argon-purged). The reactant concentrations (enzymes, substrates, and inhibitors) were as indicated in the figures, and the reactions were initiated by adding the enzyme. The pH effect was studied using 100 mM MES buffer for pH 5.5 and 5.8 and 50 mM phosphate buffer for pH 6.1−7.8 (all with 0.1 mM EDTA). Some assays were conducted at pH 6.1 with MES and phosphate buffer to confirm the noninterference of the buffer species. For the dioxygen effect study [in 50 mM phosphate buffer (pH 6.3)], the dioxygen concentration was varied by adding different volumes of air-equilibrated water to the anaerobic reaction mixture. It was assumed that air-equilibrated water has a dioxygen concentration of 245 μM (25 °C). The dioxygen concentrations assayed, 12.5, 25, 50, and 125 μM, were obtained by adding (to a final volume of 1 mL) 50, 100, 200, and 500 μL of air-equilibrated water, respectively. When indicated, 750 units/mL superoxide dismutase (SOD) was added. Aldehyde consumption and NADH consumption under the same conditions were followed spectrophotometrically, at 269 nm (DHB; $\Delta\varepsilon$ = 4710 M^{-1} cm^{-1}), 398 nm (DMAC; ε = 30500 M^{-1} cm^{-1}), and 340 nm (NADH; ε = 6100 M^{-1} cm^{-1}).

Kinetics. The steady-state apparent kinetic parameters were estimated by the Hanes method,[112] from the initial rates determined in triplicate. The kinetic mechanism type was identified with Lineweaver−Burk and Hanes plots. The real kinetic parameters were determined with secondary plots of [nitrite]/V^{app} versus [nitrite]. The pK_a values were determined by fitting the k^{app} values to the simplified eq 2, where k^{app}* is a pH-independent parameter. The dioxygen apparent competitive

DOI: 10.1021/bi500987w
Biochemistry 2015, 54, 685−710

inhibition constants (K_i^{app,O_2}) were determined with the secondary plots of K_m^{app}/V^{app} versus $[O_2]$. The steady-state rate equations indicated (eq 3 and S1 of the Supporting Information) were derived with the King−Altman method.

$$k^{app} = k^{app,*}/(1 + [H^+]/K_1 + K_2/[H^+]) \quad (2)$$

Cell Culture. HepG2 were grown in RPMI-1640 medium, with 2 mM L-glutamine, 10% FBS, 100 units/mL penicillin, and 100 mg/mL streptomicin. HMEC were grown in MCDB 131 medium, with 2 mM L-glutamine, 10% FBS, 100 units/mL penicillin, 100 mg/mL streptomicin, 10 ng/mL EGF, and 1 mg/mL hydrocortisone. Cells were kept at 37 °C, under a 5% CO_2/95% air mixture (SL ShelLab CO2 Series chamber, Sheldon Manufacturing, Inc.) and were trypsinised when they reach 80−90% confluency. Before the assays, cells were incubated (Sanyo MCO-19M chamber) at 37 °C, under hypoxic conditions, in a 5% O_2/95% N_2 mixture, for 48 h. The xanthine oxidase plus xanthine dehydrogenase activity of cells was measured as described for the purified enzymes,[108] but in the absence and presence of allopurinol, to guarantee that the activity measured is in fact due to XO and XD. Both HepG2 and HMEC displayed similar XO and XD activity (0.96 ± 0.21 microunits/mg of protein under normoxia), and their activity increased significantly (1.71 ± 0.30 microunits/mg of protein) after incubation under 5% dioxygen, for 48 h, as previously described.[73,94]

NO Measurements Recorded by Fluorescence Spectroscopy. To validate the method used to evaluate the NO generation by cell lines, purified BMXO-dependent NO formation was followed with the DAF-FM probe, under a 2% O_2/98% N_2 mixture, in RPMI-1640 medium (without sodium hydrogen carbonate and phenol red) with citrate (50 mM)/phosphate (100 mM) buffer (pH 5.0, 5.5, and 6.0). The reaction mixtures were prepared in a glovebox (homemade), under a 2% O_2/98% N_2 mixture, and all the solutions were first deoxygenated (nitrogen-purged). The dioxygen concentration in each assay was confirmed by fluorimetry with the MitoXpress probe, calibrated as described by the manufacturer. The assays were conducted in the presence of 10 μM DAF-FM and 600 units/mL SOD. All the other reactant concentrations were as indicated in the figure (in a final volume of 0.2 mL). In the end, the surface of each microplate well was covered with 100 μL of mineral oil, to prevent the diffusion of dioxygen from the atmosphere into the reaction mixture. The microplates were, then, removed from the glovebox, and the fluorescence increase was immediately followed in a microplate reader (Spectra Max Gemini EM), with excitation and emission at 495 and 515 nm, respectively. The fluorescence values observed in the presence of only DAF-FM (control/blank) were subtracted from all the other values. The fluorescence values were converted into NO concentration values using the NO donor DEA NONOate, as described by the manufacturer.

NO formation by HepG2 and HMEC was followed with the cell-permeant DAF-FM DA probe, as described above for purified BMXO, with the following modifications. DAF-FM DA (10 μM) was previously incubated with the cells, for 40 min, to allow probe internalization and hydrolysis of its acetate groups (intracellular conversion of DAF-FM DA to DAF-FM). After this incubation period, the probe excess was washed out with medium (RPMI or MCDB for HepG2 or HMEC, respectively), and the cells were allowed to incubate for more than 30 min (to guarantee the probe deacetylation by intracellular esterases). Subsequently, medium was removed, and all the reactants (as indicated in figures), except nitrite, were added. After another incubation period of 30 min, for reactant internalization, nitrite was added and, finally, the mineral oil. The microplates were, then, removed from the glovebox, and the increase in fluorescence was followed. The reactant concentrations (xanthine, nitrite, and inhibitors) were as indicated in the figures, and cell densities were 4×10^4 and 5×10^4 cells/microplate well for HepG2 and HMEC, respectively; two dioxygen concentrations were assayed, 23 and 43 μM (the dioxygen concentration was determined by fluorimetry with the MitoXpress probe; the concentration values indicated are means of at least five independent determinations, and the standard errors were <5%).

RESULTS

NO Formation during Enzymatic Nitrite Reduction. The identification of NO as the reaction product of the enzymatic nitrite reduction was conducted with a NO electrode and by EPR spectroscopy, as previously described.[43] The first approach utilizes a Clarck-type electrode (ISO-NO, WPI Inc.) that is selective for NO. The second methodology makes use of the spin-trap $(MGD)_2$-Fe, which, in the presence of NO, gives rise to a mononitrosyl−iron complex, $(MGD)_2$-Fe-NO, that exhibits a characteristic EPR triplet signal with a g value of 2.04 and a hyperfine splitting constant of 1.27 mT.[113]

As expected, both methods showed that RLXO and RLAO do reduce nitrite to NO, under anaerobic conditions, at pH 7.4, in the presence of different reducing substrate types: aldehydes and heterocyclic compounds that react at the enzyme's molybdenum center (DHB and xanthine for XO and DMAC and NMN for AO) and NADH that reacts at the FAD center (Figure 1). In addition, RLXD was also shown to catalyze the reduction of nitrite to NO (Figure 1A). In all cases, the enzymatic reduction of nitrite to NO is dependent on the concentrations of enzyme, reducing substrate, and nitrite and on time. Moreover, NO formation is absolutely dependent on the simultaneous presence of enzyme, nitrite, and a reducing substrate, as no NO formation is observed in the absence of any one of these three reactants. In all cases, NO generation was rapidly abolished upon addition of oxy-hemoglobin (Hb) (as exemplified in curve b of Figure 1B). Oxy-hemoglobin is an effective scavenger of NO, and this NO decay further confirmed that the observed curves do indeed reflect NO formation. It is noteworthy that similar results were obtained with HLXO and HLAO (Figure 1), suggesting that the rat liver enzymes provide a good model for the human counterparts.

Enzyme Redox Center Responsible for Nitrite Reduction and NO Formation. At present, it is well-established that it is the molybdenum center that directly reduces the nitrite to NO. We have previously shown (with the NO electrode) that in the presence of the molybdenum-specific XO inhibitor allopurinol there is no NO formation, regardless of the reducing substrate used (xanthine, DHB, or NADH).[43] Furthermore, by EPR spectroscopy, we have shown that the allopurinol-inhibited, fully NADH-reduced XO (that holds the Fe/S and FAD centers intact) is not able to reduce nitrite,[43] although it promptly reduces dioxygen.[86] To confirm the participation of the molybdenum center in rat and human enzyme-catalyzed nitrite reduction, several assays were conducted in the presence of allopurinol and DPI, a FAD-specific inhibitor. In addition, some assays were conducted with deflavo-RLXO and deflavo-RLAO, two enzyme forms whose FAD center was chemically removed but that retain the molybdenum and Fe/S centers intact.[86,111]

The presence of allopurinol completely inhibited the NO formation catalyzed by both native and deflavo forms of XO and

DOI: 10.1021/bi500987w
Biochemistry 2015, 54, 685−710

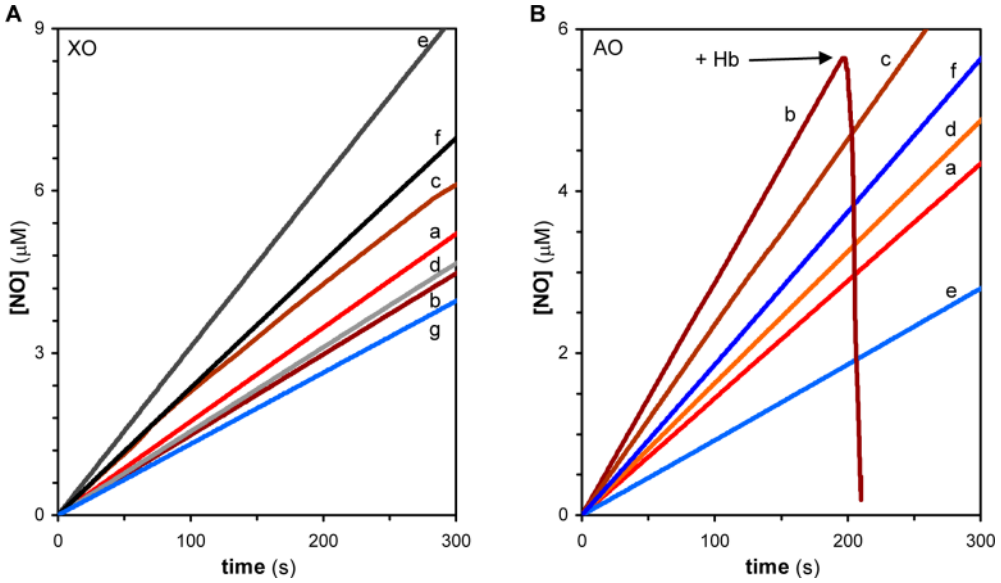

Figure 1. Time courses of XO- and AO-catalyzed NO formation evaluated with the NO-selective electrode. (A) Anaerobic NO formation during nitrite reduction was assayed, at pH 7.4, in the presence of 100 nM RLXO, 50 μM aldehyde, and 1 mM nitrite (a, red trace); 250 nM RLXO, 1 mM NADH, and 1 mM nitrite (b, dark red trace); 50 nM RLXO, 10 μM xanthine, and 1 mM nitrite (c, brown trace); 100 nM RLXD, 50 μM aldehyde, and 1 mM nitrite (d, light gray trace); 200 nM RLXD, 50 μM aldehyde, and 1 mM nitrite (e, gray trace); 100 nM RLXD, 50 μM aldehyde, and 2 mM nitrite (f, black trace); and 100 nM HLXO, 50 μM aldehyde, and 1 mM nitrite (g, light blue trace). (B) Similar assays, but with AO: 100 nM RLAO, 50 μM aldehyde, and 1 mM nitrite (a, red trace); 200 nM RLAO, 50 μM aldehyde, and 1 mM nitrite (b, dark red trace); 100 nM RLAO, 50 μM aldehyde, and 2 mM nitrite (c, brown trace); 25 nM RLAO, 400 μM NMN, and 1 mM nitrite (d, orange trace); 100 nM HLAO, 50 μM aldehyde, and 1 mM nitrite (e, light blue trace); and 200 nM HLAO, 50 μM aldehyde, and 1 mM nitrite (f, blue trace). The inhibition of NO formation in the presence of Hb is shown in curve b (the arrow indicates the addition of 100 μM Hb).

XD of rat and human liver (not shown). Moreover, the NO formation rate was directly proportional to the XO and AO AFR, a ratio that reflects the concentration of XO/AO molecules with an active molybdenum center, per FAD center.[b] In contrast, NO formation by native XO and AO in the presence of DPI or NO formation by deflavo-XO and deflavo-AO was not affected. Together, these results demonstrate that the molybdenum center, and not the FAD, is responsible for nitrite reduction and NO formation in rat and human liver enzymes.

Reduced XO was shown to be inactivated (k = 14.8 M^{-1} s^{-1}) by incubation with NO, under anaerobic conditions, and it was concluded that NO reacts with the essential terminal molybdenum sulfo group [Mo═S (Scheme 1, i)] to yield an inactive desulfo-XO form.[114] However, under our assay conditions, no inactivation was observed, either during the kinetic assays or by EPR spectroscopy (no conversion of the molybdenum rapid type 1 signal to the slow signal[115,116] was observed, during the 1 h reaction time) (data not shown; see ref 43 for EPR data). Our lack of observation of enzyme inactivation could be related to the method of NO "addition", which was a time-dependent, progressive small addition (enzymatic generation) and not in a bolus (i.e., a large amount at one time). In addition, also the fact that the enzyme is turning over, and not "trapped" in a reduced form, could delay the NO-dependent inactivation, because only reduced enzyme is inactivated.[114] The "just formed" NO would be in contact with an oxidized molybdenum, and it should rapidly diffuse away from the enzyme, directed by its concentration gradient; the subsequent inactivation would depend on NO "finding" a reduced molybdenum and on the competition with nitrite (present at a higher concentration) for that reduced molybdenum. *In vivo*, the concentration of NO formed by these enzymes should be small, and the diffusing NO should "find" numerous other biomolecules with which to react, being difficult to predict the NO concentration available to react with the molybdenum center and inactivate the enzymes.

Steady-State Kinetic Characterization of the Nitrite Reductase Activity. The nitrite reductase activity of the rat and human enzymes, at pH 7.4, was kinetically characterized following NO formation, in the presence of an aldehyde as a reducing substrate, to allow for a direct comparison between XO and AO and between RLXO and BMXO (that we have previously characterized[43]). The initial rates of NO formation were determined with the NO-selective electrode, as this method provides simple, continuous, and direct measurements of the NO concentration as a function of time. To kinetically characterize the nitrite reduction, several assays were conducted, each varying the nitrite concentration, in the presence of different constant aldehyde concentrations (as in a single substrate experiment, to determine the apparent kinetic parameters). Within the concentrations assayed, all enzymatic reactions followed Michaelis–Menten kinetics, with no evidence of substrate inhibition (no decrease in rate with increasing substrate concentrations).

In Figure 2 and Table 1 are shown the results obtained in the presence of fixed 50 μM aldehyde and of fixed 1 mM nitrite. The apparent kinetic parameters of RLXO, in the presence of 50 μM aldehyde, K_m^{app,NO_2^-} and k_{cat}^{app,NO_2^-} values of 1.92 mM and 0.545 s^{-1} (Figure 2A, diamonds, and Table 1), respectively, are in good agreement with those previously reported for BMXO (K_m^{app,NO_2^-} and k_{cat}^{app,NO_2^-} values of 2.3 mM[43] to 2.6 mM[40] and of 0.46 s^{-1}[43] to 0.85 s^{-1},[40] respectively). The parameters determined for 1 mM nitrite, $K_m^{app,ald}$ and $k_{cat}^{app,ald}$ values of 9.38 μM and 0.210 s^{-1} (Table 1), respectively, although slightly different, are also in line with those of BMXO ($K_m^{app,ald}$ and $k_{cat}^{app,ald}$ of 89.3 μM[43] to 35 μM[40] and of 0.365 s^{-1}[43] to 0.34 s^{-1},[40] respectively). The same situation is found for RLAO, with K_m^{app,NO_2^-}

DOI: 10.1021/bi500987w
Biochemistry 2015, 54, 685−710

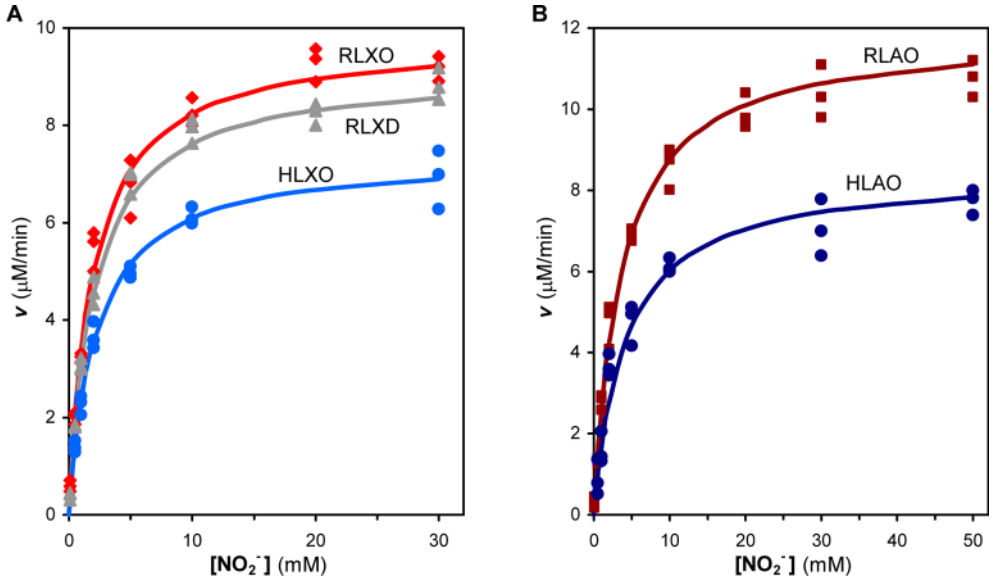

Figure 2. Kinetics of NO formation catalyzed by (A) XO and (B) AO. Initial rates of NO formation were measured with the NO-selective electrode, in the presence of 50 μM aldehyde (pH 7.4). The hyperbolic curves shown were generated with the apparent kinetic parameters listed in Table 1: RLXO (red), RLXD (gray), HLXO (blue), RLAO (dark red), and HLAO (dark blue).

and $K_m^{app,ald}$ values of 3.58 mM and 10.9 μM (Figure 2B, squares, and Table 1), respectively, for which Li et al.[44] reported values of 3.3 mM and 9.6 μM, respectively. Noteworthy, the RLAO K_m^{app,NO_2^-} is ≈2 times higher than the respective value of RLXO.

It should be emphasized that the RLXD (Figure 2A, triangles, and Table 1) displays kinetic parameters similar to those of RLXO. As far as we know, this is the first kinetic characterization of the nitrite reductase activity of the XD form, precisely the form that is believed to exist predominantly *in vivo* in mammal tissues. The two enzymatic forms, XO and XD, are known to differ only on the structure around the FAD center, showing no significant differences in the global folding at the Fe/S and molybdenum centers.[62,76,77] In addition, several kinetic studies have demonstrated that XO and XD are virtually identical with respect to the binding and catalysis of xanthine at the molybdenum center.[62,76,77] Hence, this kinetic characterization further corroborates the fact that the molybdenum center is the site of nitrite reduction. In addition, it provides an additional example of how similar are the two forms with respect to the catalysis occurring at the molybdenum center.

Of major importance are the similarities in the kinetic parameters of rat liver and human liver, HLXO (Figure 2A, circles, and Table 1) and HLAO (Figure 2B, circles, and Table 1). This similarity further supports the employment of the rat liver enzymes (whose tissue is easier to obtain and in larger amounts) as a suitable model of the human counterparts.

For the rat liver enzymes, the type of kinetic mechanism was identified using primary plots and the real kinetic parameters were determined. A Lineweaver–Burk plot with parallel lines clearly indicates that the nitrite reduction follows a "ping-pong" (substituted enzyme) mechanism, with the rate equation (eq 3).[112] Because the kinetic assays were conducted in the absence of added products, it was not possible to determine if the binding of substrates is ordered or random. However, as we have discussed for BMXO,[43] it is plausible that the aldehyde, like xanthine,[117,118] reacts only with enzyme molecules holding oxidized molybdenum, while the nitrite, probably, binds only to reduced molybdenum. Thus, it is conceivable that the aldehyde is the first substrate to bind (binding to the oxidized molybdenum), with nitrite binding in second place, only after the molybdenum had been reduced. With regard to the products, because both oxidation and reduction half-reactions occur at the molybdenum center, it seems likely that the carboxylate must first leave the enzyme for nitrite to be reduced. For these reasons, we suggest that both RLXO- and RLAO-catalyzed nitrite reduction occur through an ordered mechanism, with the aldehyde being the first substrate to bind and NO the last product to leave the enzyme (as schematically represented above eq 3).

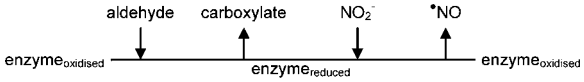

$$v^{(\text{formation NO})} = \frac{k_{cat}\,[\text{ald}]\,[NO_2^-]}{K_m^{NO2\text{-}}\,[\text{ald}] + K_m^{ald}\,[NO_2^-] + [\text{ald}]\,[NO_2^-]} \quad (3)$$

The real kinetic parameters determined (Table 1) indicate that, although the RLAO $K_m^{NO_2^-}$ value is higher (2.7 times), the RLXO and RLAO specificity for nitrite is quite similar, ≈200–275 $M^{-1}\,s^{-1}$.

Because the specificity of the enzymes for nitrite was found to be higher at acidic pH values (shown below), the real kinetic parameters were also determined at pH 6.3. At this pH, nitrite reduction was found also to follow a "ping-pong" (substituted enzyme) kinetic mechanism, but with different parameters (Table 1). As a result, the specificity of the enzymes for nitrite is considerably higher at pH 6.3 than at pH 7.4, being 2.19 and $1.64 \times 10^3\ M^{-1}\,s^{-1}$, at pH 6.3, for RLXO and RLAO, respectively. These values indicate that, under similar conditions (reducing substrates and nitrite availability), the enzyme-catalyzed reduction of nitrite to NO would be significantly higher at pH 6.3 (8 times) than at pH 7.4. This finding is of major importance for the *in vivo* role of XO/AO-dependent NO generation under the acidic conditions characteristic of ischemia, as discussed below.

With regard to the comparison of RLXO versus RLAO (Table 1), although the limiting rate of AO reaction is higher, its

DOI: 10.1021/bi500987w
Biochemistry 2015, 54, 685–710

Table 1. Kinetic Parameters of the Substrate Aldehyde

Nitrite Reduction/NO Formation in the Presence of Aldehyde and Absence of Dioxygen						
Apparent Kinetic Parameters at pH 7.4						
	for 1000 μM nitrite		for 50 μM aldehyde		for 750 μM aldehyde	
enzyme	$K_m^{app,ald}$ (μM)	k_{cat}^{app} (s^{-1})	K_m^{app,NO_2^-} (μM)	k_{cat}^{app} (s^{-1})	K_m^{app,NO_2^-} (μM)	k_{cat}^{app} (s^{-1})
RLXO	9.38	0.210	1918	0.545	3367	0.939
RLXD	9.71	0.231	2011	0.508	3321	0.903
RLAO	10.9	0.169	3585	0.661	8668	1.59
HLXO	9.58	0.203	2161	0.411	3521	0.824
HLAO	26.5	0.129	4088	0.471		
Kinetic Parameters at pH 7.4						
enzyme	$K_m^{NO_2^-}$ (μM)	K_m^{ald} (μM)	k_{cat} (s^{-1})			
RLXO	3632	43.2	0.994			
RLAO	9723	91.0	1.89			
Apparent Kinetic Parameters at pH 6.3						
	for 1000 μM nitrite		for 50 μM aldehyde		for 750 μM aldehyde	
enzyme	$K_m^{app,ald}$ (μM)	k_{cat}^{app} (s^{-1})	K_m^{app,NO_2^-} (μM)	k_{cat}^{app} (s^{-1})	K_m^{app,NO_2^-} (μM)	k_{cat}^{app} (s^{-1})
RLXO	52.3	0.898	251	0.581	603	1.32
RLXD					624	1.29
RLAO	69.6	1.07	432	0.657	1633	2.53
HLXO					665	1.20
Kinetic Parameters at pH 6.3						
enzyme	$K_m^{NO_2^-}$ (μM)	K_m^{ald} (μM)	k_{cat} (s^{-1})			
RLXO	666	78.2	1.46			
RLAO	2052	204	3.37			
Nitrite Reduction/NO Formation in the Presence of Aldehyde and Dioxygen						
Apparent Kinetic Parameters at pH 6.3						
		K_i^{app,O_2} (μM)				
enzyme	for 50 μM aldehyde	for 750 μM aldehyde	for 1500 μM aldehyde			
RLXO	24.3	42.7				
RLAO	25.2		48.8			
Dioxygen Reduction in the Presence of Aldehyde and Absence of Nitrite						
Apparent Kinetic Parameters at pH 6.3						
	for 50 μM aldehyde		for 750 μM aldehyde			
enzyme	K_m^{app,O_2} (μM)	k_{cat}^{app} (s^{-1})	K_m^{app,O_2} (μM)	k_{cat}^{app} (s^{-1})		
RLXO	27.1	1.92	50.9	3.29		
RLAO	25.1	2.70				
Kinetic Parameters at pH 6.3						
enzyme	$K_m^{O_2}$ (μM)	K_m^{NADH} (μM)	k_{cat} (s^{-1})			
RLXO	$\geq$50.9[a]	*ca* 50[b]	$\geq$3.29[a]			

[a]Assuming a "ping-pong" kinetic mechanism, for which it can be demonstrated that the apparent values tend to the real values for saturating substrate concentrations. [b]Considering the only two aldehyde concentrations to define the straight line of the Hanes plot.

superior $K_m^{NO_2^-}$ value (lower specificity for nitrite) suggests that the relative AO contribution to the NO generation would be smaller than that of XO. Nevertheless, at the same reducing substrate, nitrite, and enzyme concentrations, the amount of NO formed by both enzymes would be quite similar, e.g., 1.6−2.1 nM NO/s, for 100 nM enzyme (30 μg/mL that could simulate 30 μg/g of tissue), 10 μM nitrite (a reasonable *in vivo* value), and 50 μM aldehyde (using eq 3 and the pH 6.3 real parameters).

Role of the Reducing Substrate. Some supplementary kinetic assays were conducted with other reducing substrates, xanthine, NMN, and NADH, present at two concentrations, a low to moderate concentration and a high concentration. Although the high concentrations are not physiologically meaningful, they should create conditions closer to saturation and, thus, spurn apparent kinetic parameters closer to the real ones (assuming that all reactions follow a "ping-pong" type of mechanism).

As summarized in Table 2, all the K_m^{app,NO_2^-} values determined at pH 7.4 are in the millimolar range. For the lower reducing substrate concentrations, the values range from 1.9 to 3.0 mM, for RLXO, and from 2.0 to 3.6 mM, for RLAO, while for the higher reducing substrate concentrations, the values vary from 3.4 to 7.6 mM, for RLXO, and from 4.9 to 8.7 mM, for RLAO. The values obtained with the lower reducing substrate concentrations are in good agreement with those previously reported (2.3−2.6 mM for XO[40] and 2.7−3.3 mM for AO[44]). These results (and also the individual curves in Figure 1) demonstrate that the enzymes do catalyze the reduction of nitrite to NO in the presence of any reducing substrate (electron donor to the enzyme), regardless of its chemical nature or site of reaction with the enzymes (aldehydes, xanthine, and NMN react at the molybdenum center, while NADH reacts at the FAD center). The k_{cat}^{app} values, on the other hand, clearly follow the trend observed for the respective dioxygen reduction reaction, with the fastest reactions occurring with RLXO/xanthine and RLAO/NMN systems, as would be expected from the high XO specificity for xanthine (k_{cat} = 17.2 s^{-1}, and K_m^{xant} = 1.8 μM[109]) and AO specificity for NMN (k_{cat} = 12.7 s^{-1}, and K_m^{NMN} = 400 μM[110,111]).

DOI: 10.1021/bi500987w
Biochemistry 2015, 54, 685−710

Table 2. Kinetic Parameters with Substrates NADH, Xanthine, and NMN

Nitrite Reduction/NO Formation in the Presence of NADH and Absence of Dioxygen				
Apparent Kinetic Parameters at pH 7.4				
	for 1000 μM nitrite		for 1000 μM NADH	
enzyme	$K_m^{app,NADH}$ (μM)	k_{cat}^{app} (s^{-1})	K_m^{app,NO_2^-} (μM)	k_{cat}^{app} (s^{-1})
RLXO	259	0.0739	2133	0.185
	for 7500 μM nitrite		for 10,000 μM NADH	
	$K_m^{app,NADH}$ (μM)	k_{cat}^{app} (s^{-1})	K_m^{app,NO_2^-} (μM)	k_{cat}^{app} (s^{-1})
	731	0.249	3989	0.331
Kinetic Parameters at pH 7.4				
enzyme	$K_m^{NO_2^-}$ (μM)	K_m^{NADH} (μM)	k_{cat} (s^{-1})	
RLXO	$\geq$3989[a]	$\geq$731[a]	$\geq$0.331[a]	
Apparent Kinetic Parameters at pH 6.3				
	for 1000 μM nitrite		for 1000 μM NADH	
enzyme	$K_m^{app,NADH}$ (μM)	k_{cat}^{app} (s^{-1})	K_m^{app,NO_2^-} (μM)	k_{cat}^{app} (s^{-1})
RLXO	1504	0.189	352	0.100
	for 7500 μM nitrite		for 10,000 μM NADH	
	$K_m^{app,NADH}$ (μM)	k_{cat}^{app} (s^{-1})	K_m^{app,NO_2^-} (μM)	k_{cat}^{app} (s^{-1})
	3153	0.398	1117	0.327
Kinetic Parameters at pH 6.3				
enzyme	$K_m^{NO_2^-}$ (μM)	K_m^{NADH} (μM)	k_{cat} (s^{-1})	
RLXO	$\geq$1117[a]	$\geq$3153[a]	$\geq$0.398[a]	
Nitrite Reduction/NO Formation in the Presence of NADH and Dioxygen				
Apparent Kinetic Parameters at pH 6.3				
	for 1000 μM NADH		for 10,000 μM NADH	
enzyme	K_i^{app,O_2} (μM)		K_i^{app,O_2} (μM)	
RLXO	32.5		34.0	
Dioxygen Reduction in the Presence of NADH and Absence of Nitrite				
Apparent Kinetic Parameters at pH 6.3				
	for 50 μM NADH		for 500 μM NADH	
enzyme	K_m^{app,O_2} (μM)	k_{cat}^{app} (s^{-1})	K_m^{app,O_2} (μM)	k_{cat}^{app} (s^{-1})
RLXO	32.8	0.0412	45.9	0.0551
Kinetic Parameters at pH 6.3				
enzyme	$K_m^{O_2}$ (μM)	K_m^{NADH} (μM)	k_{cat} (s^{-1})	
RLXO	$\geq$45.9[a]	~23[b]	$\geq$0.055[a]	
Nitrite Reduction/NO Formation in the Presence of Xanthine or NMN and Absence of Dioxygen				
Apparent Kinetic Parameters at pH 7.4				
	for 10 μM xanthine		for 100 μM xanthine	
enzyme	K_m^{app,NO_2^-} (μM)	k_{cat}^{app} (s^{-1})	K_m^{app,NO_2^-} (μM)	k_{cat}^{app} (s^{-1})
RLXO	2996	2.32	7601	5.87
	for 400 μM NMN		for 4000 μM NMN	
enzyme	K_m^{app,NO_2^-} (μM)	k_{cat}^{app} (s^{-1})	K_m^{app,NO_2^-} (μM)	k_{cat}^{app} (s^{-1})
RLAO	2039	2.03	4853	4.89

[a]Assuming a "ping-pong" kinetic mechanism, for which it can be demonstrated that the apparent values tend to the real values for saturating substrate concentrations. [b]Considering the only two NADH concentrations to define the straight line of the Hanes plot.

The apparent kinetic parameters of RLXO-catalyzed nitrite reduction by NADH were also determined at pH 6.3 (Table 2). It is expected that all parameters, $K_m^{NO_2^-}$, K_m^{NADH}, and k_{cat}, change with the pH; hence, 1 and 10 mM NADH and 1 and 7.5 mM nitrite would represent different percentages of saturation at different pH values. With this limitation in mind, it can be suggested that, when the pH is decreased from 7.4 to 6.3, $K_m^{NO_2^-}$ decreases and K_m^{NADH} and k_{cat} increase. Therefore, it can be suggested that the NADH-dependent nitrite reduction would follow the same trend as the aldehyde-dependent reaction; that is, the XO specificity for nitrite would be higher at pH 6.3 than at pH 7.4.

However, compared to that of aldehyde, the level of NADH-dependent NO formation is considerably lower. For 100 nM enzyme and 10 μM nitrite, 1 mM NADH and 50 μM aldehyde would drive NO formation at 0.28 and 2.2 nM/s, at pH 6.3, and at 0.086 and 0.283 nM/s, at pH 7.4, respectively (using the respective apparent constants at both pH values).

Effect of pH on Nitrite Reductase Activity. During an ischemic event, the pH decreases to values as low as 6.0−5.5 (acidosis).[119−124] Therefore, to evaluate the relative physiological significance of XO/AO-dependent NO formation, it is crucial to characterize how the pH modulates nitrite reductase activity. Previous discrete (single nitrite concentration) basic kinetic assays have suggested that NO formation would be favored at acidic pH values,[39,40,44] but no detailed kinetic characterization had yet been undertaken.

The effect of pH on the nitrite reductase activity of rat liver enzymes was studied in the presence of a high aldehyde concentration (750 μM DHB and 1500 μM DMAC, for RLXO and RLAO, respectively). The characterization of the effects of pH on real kinetic parameters would consume a large amount of enzyme, which was not viable. While high aldehyde concentrations may not be physiologically meaningful, with their use we aimed (i) to obtain apparent kinetic parameters closer to the real ones (assuming that the "ping-pong" type of mechanism determined at pH 6.3 and 7.4 does not change over the pH range studied) and (ii) simultaneously to guarantee that saturation or near saturation is achieved at all pH values (because the K_m^{ald} value would be expected to vary with pH).

The pH dependence of the RLXO and RLAO specificity constant for nitrite (k^{app,NO_2^-}, calculated as the $k_{cat}^{app,NO_2^-}/K_m^{app,NO_2^-}$ ratio) was found to result in a bell-shaped curve, characterized by apparent pK_a values of 5.9 and 6.8, for RLXO, and 6.0 and 7.0, for RLAO (Figure 3, red diamonds and dark red squares, for RLXO and RLAO, respectively). The RLXD apparent kinetic parameters were also studied at some pH values (Figure 3, red triangles, and Table 1) and found to be in accordance with the RLXO ones, as would be expected given the similarities at the molybdenum domain of both enzyme forms (discussed above in steady-state kinetic characterization). Also, the HLXO apparent kinetic parameters were studied (Figure 3, red circles, and Table 1). The agreement found between the kinetic parameters of human and rat liver XO is highly significant for the employment of the rat liver enzymes as a suitable model of the human counterparts and is of major importance for the suggested role of HLXO and HLAO in NO generation.

Hence, with all enzymes (XO/XD and AO), nitrite reduction is favored under lower-pH (<7) conditions, exhibiting the highest specificity constant for nitrite at pH ≈6.3−6.5. The specificity constant for nitrite is formally the apparent pseudo-first-order rate constant,[112] and this pH dependence is particularly relevant, because it refers to the reaction rate when nitrite is present at a concentration much lower than its K_m and the *in vivo* nitrite concentration (<20 μM[125−128]) is much lower than the $K_m^{NO_2^-}$ values reported by us and others. If these enzymes are to be relevant *in vivo* NO sources under ischemia, they should display high pseudo-first-order rate constants at the acidic pH characteristic of hypoxia; only in this way can the enzymes overcome the constraint imposed by the high $K_m^{NO_2^-}$ values and/or low nitrite availability. Therefore, with these results, it is clear that the ability of the enzymes to trigger NO formation is considerably greater under the acidic conditions characteristic of ischemia than at the normal pH of 7.4.

DOI: 10.1021/bi500987w
Biochemistry 2015, 54, 685−710

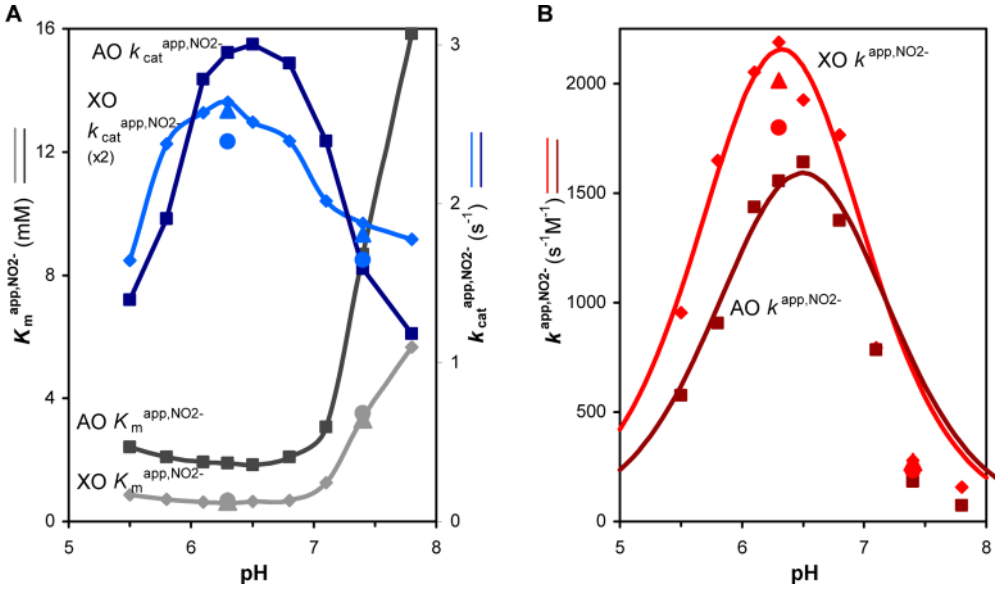

Figure 3. pH dependence of the apparent kinetic parameters of XO and AO. Apparent kinetic parameters of RLXO (light colors, diamonds) and RLAO (dark colors, squares) were determined for the pH values indicated. Some values of RLXD (light colors, triangles) and HLXO (light colors, circles) are also represented. The k_{cat}^{app,NO_2^-} values of RLXO, RLXD, and HLXO were multiplied by 2 to facilitate the comparison with the values of AO: K_m^{app,NO_2^-} (RLXO), light gray diamonds; K_m^{app,NO_2^-} (RLXD), light gray triangles; K_m^{app,NO_2^-} (RLAO), dark gray squares; K_m^{app,NO_2^-} (HLXO), light gray circles; k_{cat}^{app,NO_2^-} (RLXO), light blue diamonds; k_{cat}^{app,NO_2^-} (RLXD), light blue triangles; k_{cat}^{app,NO_2^-} (RLAO), dark blue squares; k_{cat}^{app,NO_2^-} (HLXO), light blue circles; $k^{NO_2^-}$ (RLXO), red diamonds; $k^{NO_2^-}$ (RLXD), red triangles; $k^{NO_2^-}$ (RLAO), dark red squares; $k^{NO_2^-}$ (HLXO), red circles.

Apart from contributing to the evaluation of the relative physiological significance, one of the principal reasons to study the effects of pH on specificity constants is to determine pK_a values that allow one to deduce the chemical nature of the groups on the free enzyme and/or free substrate that participate in catalysis.[112] Thus, inspection of Figure 3 suggests that nitrite reduction would depend on the deprotonation of a group with a pK_a of ≈6 and on the protonation of another group with a pK_a of ≈7. However, the identity of such ionizable groups is difficult to predict. The XO-catalyzed hydroxylation reactions are well-characterized, and the bell-shaped pH curves of k have been interpreted as arising from the deprotonation of a key glutamate residue [BMXO Glu_{1261} (see Scheme 1, i), with a pK_a of ≈6.3−6.6] and from the protonation of the substrate (e.g., xanthine with a pK_a of ≈7.4[129] or DHB with a pK_a of ≈8.6[130]). Given that the reducing substrates used in this work have pK_a values of >7 and nitrite has a pK_a of 3.2, it is not straightforward to interpret the observed pH dependence of nitrite reduction.

Nevertheless, a bell-shaped pH curve may also arise from a single ionizable group that is required in different protonation states in two steps of the catalytic cycle, that is, e.g., a single group that must be deprotonated in the first step and protonated in the second.[112] In the context of XO/AO, it can be hypothesized that such an ionizable group is the conserved key glutamate residue (BMXO Glu_{1261}). (i) In the first part of the catalytic cycle (oxidation half-reaction), the deprotonated glutamate functions as a base and assists the Mo−O^- nucleophilic attack on the carbon center to be hydroxylated (see footnote *e*; Scheme 1, ii, a → c),[58−64] while (ii) during the nitrite reduction part (reduction half-reaction), the same glutamate residue, but at this point protonated, is well positioned to act as the proton donor required to reduce nitrite (eq 1 and Scheme 1, ii, e → f). The rate equation (eq S1) derived for such a mechanism (Scheme S1 of the Supporting Information) shows that the pH dependence of the kinetic parameters (k_{cat}, K_m, and k) is extremely complex. The specificity constant for nitrite is not defined by only the ionization constants of the free enzyme and/or free substrate, as is usually the case. On the contrary, the specificity constant is a complex function that includes the ionization constants of free enzyme forms and substrate, intermediates, and product-bound enzyme forms (eq S1). Moreover, the pK_a values experimentally determined are not ionization constants at all but, instead, a constant or combination of constants distorted by rate constants (eq S1). In spite of it is complexity, eq S1 yields pH curves with profiles (Figure S1 of the Supporting Information) similar to those observed here (Figure 3) and, thus, supports the hypothesis for the dual role of the conserved glutamate residue.

The K_m^{app,NO_2^-} pH dependence shows that the K_m^{app,NO_2^-} values of both enzymes decrease markedly as the pH is lowered, reaching a plateau for pH ≤6.8, of ≈600−800 μM and ≈1.9−2.1 mM for RLXO and RLAO, respectively (Figure 3). With regard to the k_{cat}^{app,NO_2^-} curves, they are similar to the $k^{NO_2^-}$ curves, indicating that also the highest possible rate of NO formation occurs at pH values of ≈5.8−6.8. These profiles could be rationalized assuming (Scheme 1, ii) that, under acidic conditions, the key glutamate residue is favorably protonated, which would favor the nitrite protonation step and, consequently, increase the reduction half-reaction rate and, eventually, the k_{cat}. Concomitantly, the reaction would require lower nitrite concentrations to be driven (lower K_m). When the pH is further lowered (<5.5), although the nitrite reduction would be (as suggested) favored, the oxidation half-reaction would be seriously unfavored, because of the marked decrease in the level of deprotonated glutamate. This would result in a clear decrease in the number of reduced enzyme molecules to react with nitrite and, consequently, in k_{cat} values.

Regardless of the kinetic mechanisms responsible for those pH effects, the K_m^{app,NO_2^-} decrease (≈5−6-fold) under acidic conditions is particularly significant. The pseudo-first-order rate constant (specificity constant) for nitrite reaches its maximal value under acidic conditions, and the K_m is minimized. In light of

DOI: 10.1021/bi500987w
Biochemistry 2015, 54, 685−710

the low *in vivo* nitrite concentration (<20 μM[125−128]), the smaller the $K_m^{NO_2^-}$ value, the higher the probability of XD/XO/AO to contribute to *in vivo* NO formation (because lower nitrite concentrations would be needed to drive a similar rate of NO generation).

The XO $K_m^{NO_2^-}$ value on the order of millimolar is one of the strongest arguments against its involvement in *in vivo* NO formation, but those extremely high K_m values were determined at pH 7.4 and than extrapolated to apply to acidic conditions, under which only discrete (single-concentration) kinetic assays were conducted. The kinetic characterization presented here indicates that the discrepancy between $K_m^{NO_2^-}$ and *in vivo* nitrite concentration is pH-dependent, being minimized under acidic conditions and not being as high as previously envisaged [i.e., K_m^{app,NO_2^-} values of ≈600 μM (pH 6.3) and not ≈3 mM (pH 7.4)].

In this context, it should be noted that it would not be physiologically conceivable to form NO at concentrations on the same order of magnitude as the *in vivo* nitrite concentrations, that is, at the micromolar level. NO performs its functions at low nanomolar concentrations; at micromolar concentrations, controlling the specificity of NO signaling and, most importantly, its toxicity would not be achievable. Thus, it is not reasonable that any nitrite-dependent NO formation pathway produces NO in concentrations equimolar to those of nitrite.

Together (k_{cat}, K_m, and k), the observed pH dependencies suggest that these enzymes would be able to trigger NO formation *in vivo* and the amount of NO formed would be considerably larger under the acidic conditions characteristic of ischemia, compared to the amount at normal pH 7.4. Also the induction of ischemia that reduces the level of accumulation of substrates would contribute to NO generation by "charging" the enzymes with the electrons necessary to reduce nitrite (eq 1). Overall, these findings support the physiological relevance of XO/AO-dependent NO formation.

Effect of Dioxygen on Nitrite Reductase Activity. At present, it is clear that, *in vitro*, under anaerobic conditions, XD, XO, and AO do catalyze the reduction of nitrite to NO (this work and previous works[37−44]). However, and as can be anticipated, the "classic" oxidizing substrates, dioxygen and NAD^+, should act as strong competitive inhibitors of NO formation, either *in vitro* or *in vivo*, because they efficiently consume the electrons needed to reduce nitrite (eq 1). In fact, the kinetic characterization conducted by Li et al.[41] has already shown the dioxygen effect on BMXO-catalyzed NO formation at pH 7.4, as well as a few other single-concentration inhibition studies.[39,44] Therefore, it is also critical to characterize how dioxygen inhibits the nitrite reductase activity of liver enzymes. In addition, also the NAD^+ inhibition of liver XD-dependent NO formation should be evaluated. However, such characterization is outside the scope of this work, being the aim of future work. Because it is physiologically more meaningful to conduct this characterization under the acidic conditions characteristic of ischemia and because the specificity of enzymes for nitrite is higher at pH ≈6.3−6.5, the dioxygen effect study was undertaken at pH 6.3.

Dioxygen interferes with NO at different levels (Scheme 2). (i) Dioxygen is efficiently reduced at the enzyme's FAD center (eq 4) and rapidly consumes the electrons derived from the reducing substrates. Consequently, dioxygen readily decreases the concentration of enzyme molecules with reduced molybdenum available to react with nitrite, thus decreasing (inhibiting) NO formation. Theoretically, it can be demonstrated that the dioxygen competitive inhibition constant (K_i^{app,O_2}) is formally

Scheme 2. Effects of Dioxygen on the NO Status in the XO and AO Systems[a]

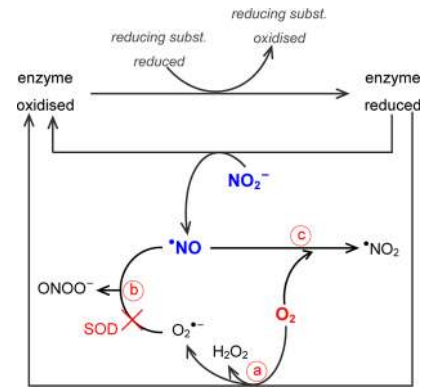

[a]Dioxygen interferes with NO at different levels. (a) Dioxygen is efficiently reduced by the enzymes, consuming the electrons derived from the reducing substrates. As a result, dioxygen readily decreases the concentration of reduced enzymes to react with nitrite, thus decreasing (inhibiting) NO formation. (b) Simultaneously, the superoxide anion radical formed reacts with NO to yield peroxynitrite. This dioxygen effect can be counteracted by the presence of SOD. (c) In addition, dioxygen can also react directly with NO to yield nitrogen dioxide radical and other products.

equal to K_m^{app,O_2} and that the reaction rate is expressed by eq 5, where K_m^{app,NO_2^-} and K_m^{app,O_2} are the apparent values determined for the same reducing substrate, present at the same constant concentration, but in the absence of dioxygen (K_m^{app,NO_2^-}) and nitrite (the K_m^{app,O_2}), respectively.[c,112] (ii) At the same time, the superoxide anion radical formed (eq 4) reacts with NO to yield peroxynitrite, in a diffusion-controlled reaction (eq 6; $k \approx 10^9$−10^{10} M^{-1} s^{-1}).[6,131] This effect can be counteracted by the presence of superoxide dismutase (SOD; eq 7; $k \approx 2 \times 10^9$ M^{-1} s^{-1}[1132,133]), but in this case, the dioxygen is partially restored in the system. (iii) In addition, dioxygen can also react directly with NO, although in a comparatively slow reaction ($k \approx 10^6$–10^7 M^{-2} s^{-1}), to yield different products (eq 8 → eq 10). This dioxygen effect cannot be experimentally counteracted. Therefore, dioxygen is able to decrease the amount of NO formed (i) and the amount of NO available to be detected (ii and iii). The simultaneous occurrence of these two types of effects complicates the interpretation of the effect of dioxygen on nitrite reductase activity and probably explains some inconsistencies found in the literature.

$$O_2 + e^- + H^+ \xrightarrow{\text{(XD/XO/AO) FAD}} n\,O_2^{\bullet-} + m\,H_2O_2 \quad (4)$$

$$v^{(\text{NO formation/presence O2})} = \frac{k_{cat}^{app}\,[NO_2^-]\,[\text{enzyme}]}{K_m^{app,NO2-}\left[1 + \frac{[O_2]}{K_m^{app,O2}}\right] + [NO_2^-]} \quad (5)$$

$$^{\bullet}NO + O_2^{\bullet-} \longrightarrow ONOO^- \quad (6)$$

$$2\,O_2^{\bullet-} + 2H^+ \xrightarrow{\text{SOD}} H_2O_2 + O_2 \quad (7)$$

$$2\,^{\bullet}NO + O_2 \rightleftharpoons 2\,^{\bullet}NO_2 \quad (8)$$

$$^{\bullet}NO + {}^{\bullet}NO_2 \rightleftharpoons N_2O_3 \quad (9)$$

$$N_2O_3 + H_2O \longrightarrow 2NO_2^- + 2H^+ \quad (10)$$

Three assays types were employed to access the extent of each type of dioxygen effect. The first were assays to evaluate the direct reaction of NO with dioxygen (eq 8) under our assay conditions. The amount of NO consumed in this reaction is dependent on

DOI: 10.1021/bi500987w
Biochemistry 2015, 54, 685−710

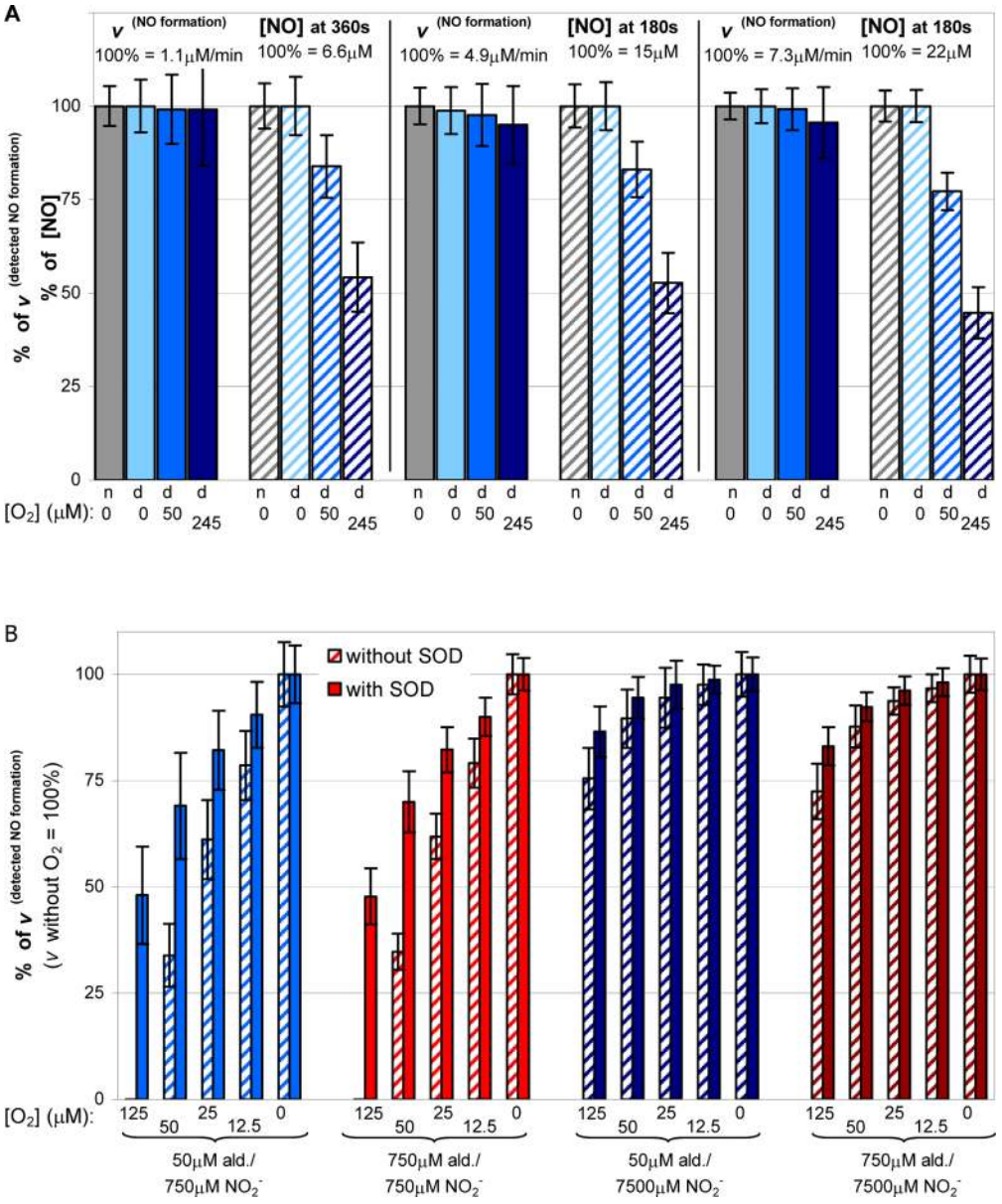

Figure 4. Effects of dioxygen on NO formation by the XO and AO systems. Evaluation of direct reaction of NO with dioxygen (A) and with superoxide radical (B). (A) The initial rate of NO formation and NO concentration at the indicated times (180 and 360 s) were measured in the presence of 750 μM aldehyde, 100 nM RLXO, and 100 μM (first and second groups of bars), 1000 μM (third and fourth groups of bars), and 7000 μM nitrite (fifth and sixth groups of bars). The measurements were taken with native RLXO under anaerobic conditions (gray bars, labeled n0), deflavo-RLXO under anaerobic conditions (light blue bars, labeled d0), deflavo-RLXO with 50 μM dioxygen (blue bars, labeled d50), and deflavo-RLXO with 245 μM dioxygen (dark blue bars, labeled d245). The rate values are represented by filled bars, while the NO concentration values are represented by striped bars. At the top of each group of bars is indicated the rate of NO formation and NO concentration measured with the native enzyme under anaerobic conditions. These values were taken to be 100%. (B) The initial rate of NO formation was measured in the presence of the indicated nitrite, dioxygen and aldehyde concentrations, in the absence (striped bars) and presence (filled bars) of SOD, and with 100 nM RLXO. The NO formation rate observed under anaerobic conditions was taken to be 100% for each group of bars.

the square of its concentration. For example, for a fixed NO concentration of 5 μM, NO consumption of ~7.5 and ~37%/min would be expected in the presence of 50 and 245 μM dioxygen, respectively (with a k of 5×10^6 M^{-2} s^{-1}), but for a fixed concentration of 15 μM, NO consumption is expected to be ~22.5 and >100%/min for 50 and 245 μM dioxygen, respectively. These high values of NO consumption would hamper the study of dioxygen inhibition (they would yield artificially high inhibition values).

To provide a measure of the direct reaction of NO with dioxygen under our assay conditions, we conducted some aerobic assays with deflavoenzymes (Figure 4A). Deflavoenzymes are not able to reduce dioxygen; therefore, in their presence, there will be no dioxygen enzyme inhibition (eq 5) or NO consumption by superoxide (eq 6). For example, the third and fourth groups of bars in Figure 4A show that the measured NO formation rate decreases only 3−5% in the presence of 50−245 μM dioxygen, assuming as 100% the deflavo-RLXO rate of 4.9 μM/min under anaerobic conditions. However, reaction for only 3 min is sufficient to decrease the amount of NO detected to 17 and 47% in the presence of 50 and 245 μM dioxygen, respectively, compared to a NO concentration

DOI: 10.1021/bi500987w
Biochemistry 2015, 54, 685−710

of ≈15 μM under anaerobic conditions (=100%). The presence of SOD does not change the rate or NO concentration, as expected for a system in which no superoxide is formed. Overall, the results in Figure 4A show that the decrease in the level of NO due to the NO/O_2 direct reaction is not as high as would be predicted by the simple calculation of $k[NO]^2[O_2]$. On the other hand, if only initial rates are considered, as in this work, the NO/O_2 direct reaction can be neglected (considered to be within the experimental error). Moreover, under nonanaerobic conditions, the reaction of NO with superoxide (eq 6), which is considerably faster, would render the flux through the NO/O_2 reaction relatively small. However, *in vivo*, under nonanoxic conditions, the NO/O_2 direct reaction probably cannot be neglected, although this is also a constraint for NOS enzymes themselves, which must catalyze NO formation in the presence of dioxygen (one of the reaction substrates).

The second were assays with native enzymes in the presence of dioxygen but in the absence of SOD. The aim of these assays was to provide a measure of NO consumption by superoxide radical (eq 6), by comparison with assays in the presence of SOD, and, thus, to validate the assays with SOD.

In the presence of dioxygen and in the absence of SOD, it is possible to detect NO. However, the detected NO formation rate (and NO concentration) is dependent on the concentrations of nitrite and dioxygen (Figure 4B). For a limiting nitrite concentration [750 μM (blue and red bars in Figure 4B)], the differences between the values obtained with and without SOD are large, indicating a relatively high level of formation of superoxide. The extreme case was observed in the presence of 125 μM dioxygen (first bars in each group of Figure 4B). At this dioxygen concentration, the RLXO time courses displayed an initial lag phase where no NO is detected ($v = 0$). The extent of this lag phase is related to the aldehyde concentration, being >900 and ≈350 ± 50 s for 50 and 750 μM aldehyde, respectively. However, in the presence of SOD, no lag phase was observed (v of 1.25 ± 0.14 and 2.10 ± 0.17 for 50 and 750 μM aldehyde, respectively), indicating that NO is being formed, but it is not detected in the absence of SOD, because it is being consumed by the relatively high superoxide concentration. For a saturating nitrite concentration [7500 μM (dark blue and dark red bars in Figure 4B)], no lag phase was observed and the differences between the values obtained with and without SOD, at all dioxygen concentrations, are smaller. These results are explained by the competition between nitrite and dioxygen for reduced enzyme, which would be more favorable to nitrite at higher concentrations. Concomitantly, the amount of superoxide formed would be smaller, and for that reason, the difference "with and without SOD" is also lower.

In addition, the aldehyde concentration modulates the real and detected NO formation rates. A higher aldehyde concentration allows for a higher NO formation rate, in the presence and absence of SOD. For example, with RLXO, for 50 μM dioxygen and 750 μM nitrite, the detected NO formation is 0.854 ± 0.10 and 1.53 ± 0.14 μM/min, in the absence of SOD, and 1.81 ± 0.15 and 3.17 ± 0.13 μM/min, in the presence of SOD, for 50 and 750 μM aldehyde, respectively.

In summary, NO consumption by superoxide would be greater in the presence of a limiting nitrite concentration, regardless of the dioxygen concentration, because the competition between nitrite and dioxygen is unfavorable to nitrite and more superoxide is formed.

The third are assays with native enzymes in the presence of dioxygen and SOD, to evaluate the dioxygen inhibition of NO formation (eq 5). As discussed above, dioxygen inhibition is dependent not only on nitrite and dioxygen concentrations but also on the aldehyde concentration. Hence, the inhibition study was conducted with two extreme aldehyde concentrations, one close to the K_m^{ald} value and the other saturating, to characterize how the aldehyde concentration influences dioxygen inhibition.

With both RLXO (Figure 5A,B) and RLAO (Figure 5C,D), for nitrite concentrations lower than the $K_m^{NO_2^-}$, dioxygen inhibition is lower at the higher aldehyde concentration. Thus, the levels of inhibition of the RLXO-catalyzed 100 μM nitrite reduction with 12.5 and 125 μM dioxygen are 23.0 ± 0.8 and 73.4 ± 4.1%, respectively, in the presence of 50 μM aldehyde, while in the presence of 750 μM aldehyde, the levels of inhibition are only 15.9 ± 0.6 and 67.8 ± 3.2%, respectively. For RLAO, the corresponding values are 26.8 ± 0.9 and 75.5 ± 4.3% and 14.7 ± 0.7 and 65.1 ± 4.0% for 50 and 1500 μM aldehyde, respectively. For nitrite concentrations higher than the $K_m^{NO_2^-}$, the aldehyde concentration effect is not pronounced and the dioxygen inhibition is weaker. For RLXO-catalyzed 7500 μM nitrite reduction or RLAO-catalyzed 15000 μM nitrite reduction, dioxygen concentrations of 12.5 and 125 μM cause an inhibition of only ≈2 and ≈15−20%, respectively, in the presence of both aldehyde concentrations. It is noteworthy that with the "standard" enzyme concentration (100 nM) used throughout this work it is possible to detect NO formation with only 25 μM nitrite (Figure 5, dark red lines), in the presence of dioxygen concentrations as high as 50 μM, that is, at the normal (normoxic) tissue dioxygen concentrations.[134] The RLXO-catalyzed NO formation rates are 0.121 ± 0.021 and 0.166 ± 0.019 μM/min with 50 and 750 μM aldehyde, respectively, which correspond to inhibitions of ≈60 and ≈50%, respectively. For higher dioxygen concentrations, although NO is formed, the initial rate of its formation is too small to be accurately measured with this enzyme concentration (only for higher reactions times, NO reaches concentration values that can be reproducibly measured).

These observations are especially relevant for the *in vivo* role of XO/AO-dependent NO generation under ischemia. (i) The reducing equivalents are expected to accumulate, and thus, enzyme saturating conditions could occur, which would favor nitrite reduction and also lead to lower dioxygen inhibitions. (ii) Physiologically meaningful nitrite concentrations could trigger NO formation, even in the presence of dioxygen.

To have a quantitative measure of dioxygen inhibition, the K_i^{app,O_2} values were determined. For that purpose, the apparent kinetic parameters for nitrite, for each dioxygen concentration, were first determined. As expected for a competitive inhibition, the k_{cat}^{app,NO_2^-} values do not change significantly with the dioxygen concentration, at each aldehyde concentration. However, the K_m^{app,NO_2^-} values increased with increasing dioxygen concentrations. For RLXO, the K_m^{app,NO_2^-} values were found to be 251, 361, 478, 752, and 1499 μM for 0, 12.5, 25, 50, and 125 μM dioxygen and 50 μM aldehyde, respectively, and 603, 747, 887, 1248, and 2289 μM for 0, 12.5, 25, 50, and 125 μM dioxygen and 750 μM aldehyde, respectively. For RLAO, the K_m^{app,NO_2^-} values were 432, 588, 872, 1333, and 2472 μM for 0, 12.5, 25, 50, and 125 μM dioxygen and 50 μM aldehyde, respectively, and 1814, 2038, 2379, 3018, and 5583 μM for 0, 12.5, 25, 50, and 125 μM dioxygen and 1500 μM aldehyde, respectively. The K_i^{app,O_2} values were subsequently determined (with secondary plots of K_m^{app}/V^{app} vs $[O_2]$) to be 24.3 and 42.7 μM for RLXO and 50 and 750 μM aldehyde, respectively,

DOI: 10.1021/bi500987w
Biochemistry 2015, 54, 685−710

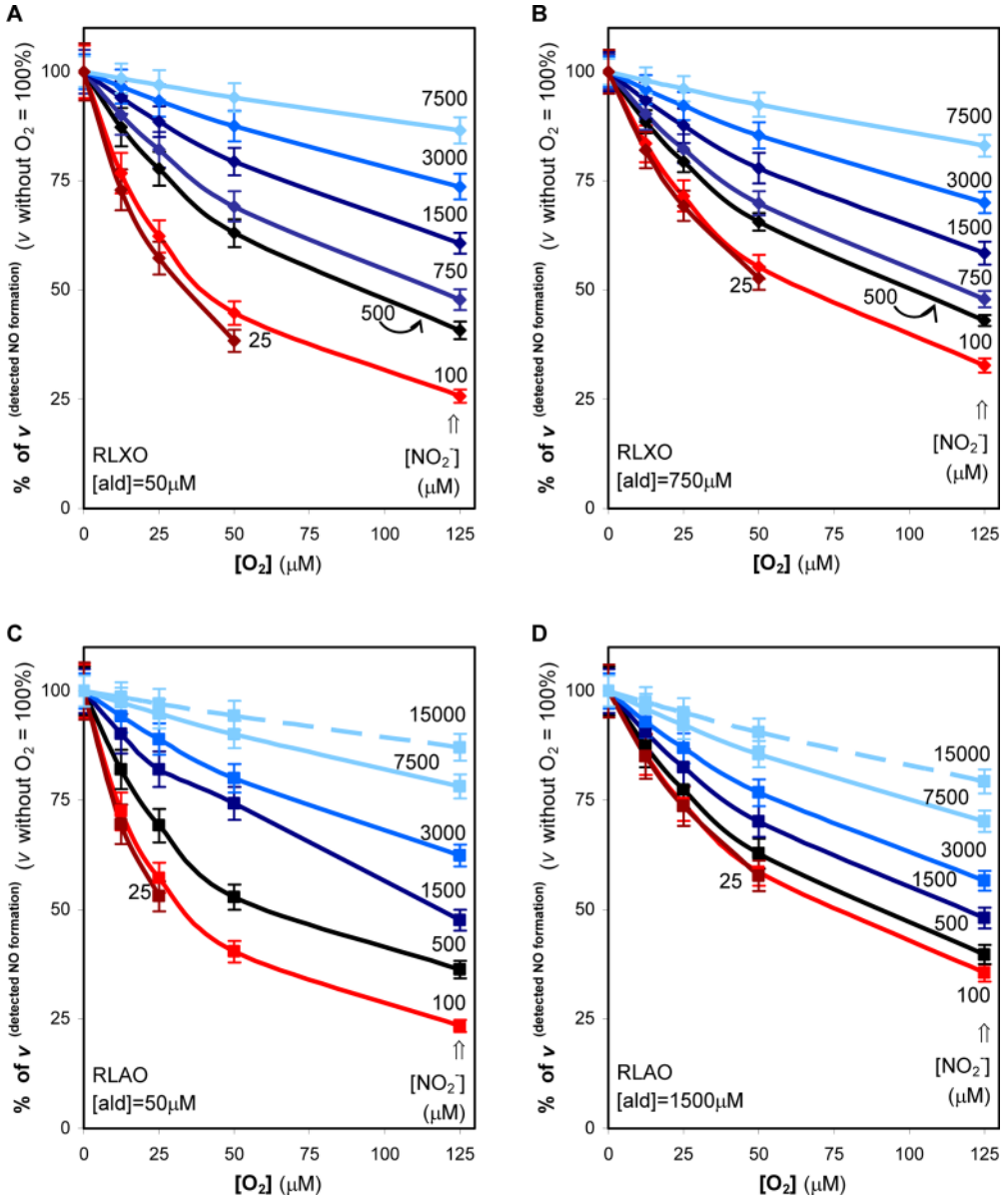

Figure 5. Dioxygen inhibition of RLXO-catalyzed (A and B) and RLAO-catalyzed (C and D) NO formation. The initial rate of NO formation was measured in the presence of the indicated nitrite, dioxygen, and aldehyde concentrations with 100 nM RLXO or RLAO in the presence of SOD. The NO formation rate observed under anaerobic conditions was taken to be 100% in each case.

and 25.2 and 48.8 μM for RLAO and 50 and 1500 μM aldehyde, respectively (Table 1).

It is noteworthy that the K_i^{app,O_2} values obtained are within the range of *in vivo* tissue dioxygen concentrations ($\leq$50 μM, from normoxia to hypoxia[134]), which suggests that *in vivo* NO formation could be fine-tuned by dioxygen availability (in opposition to no NO formation in the presence of dioxygen). Moreover, these results demonstrate that the aldehyde concentration present does have a marked effect on the K_i^{app,O_2} value, suggesting also that the *in vivo* available reducing substrate concentration could control NO formation through modulation of dioxygen inhibition.

The determined K_i^{app,O_2} values also allowed us to reach conclusions about the dioxygen-dependent reactions that can consume the enzymatically generated NO (reactions 7 and 9). As described above (also reasoning in footnote *c*), in the absence of secondary reactions that consume the enzymatically generated NO, it can be demonstrated that the K_i^{app,O_2} is formally equal to the K_m^{app,O_2} for the reaction of aldehyde with oxygen, in the absence of nitrite. Hence, for comparison, the K_m^{app,O_2} values were also determined. The values obtained are in good agreement with the respective K_i^{app,O_2} values: 27.1 and 50.9 μM for RLXO and 50 and 750 μM aldehyde, respectively, and 25.1 μM for RLAO and 50 μM aldehyde (Table 1). Therefore, in the presence of SOD, the extension of the dioxygen-dependent reactions that can consume the enzymatically generated NO is relatively small, under our assay conditions.

Finally, the determined K_i^{app,O_2} values would have allowed us to determine the real $K_i^{O_2}$ values, if more aldehyde concentrations were assayed. (If the only two aldehyde concentrations are considered to define the straight line of the Hanes plot, $K_i^{O_2}$ values of 45.2 and 50.4 μM would be obtained for RLXO and RLAO, respectively.) Nevertheless, if one assumes a "ping-pong" kinetic mechanism (for which it can be demonstrated that the apparent values tend to the real values for saturating aldehyde

DOI: 10.1021/bi500987w
Biochemistry 2015, 54, 685−710

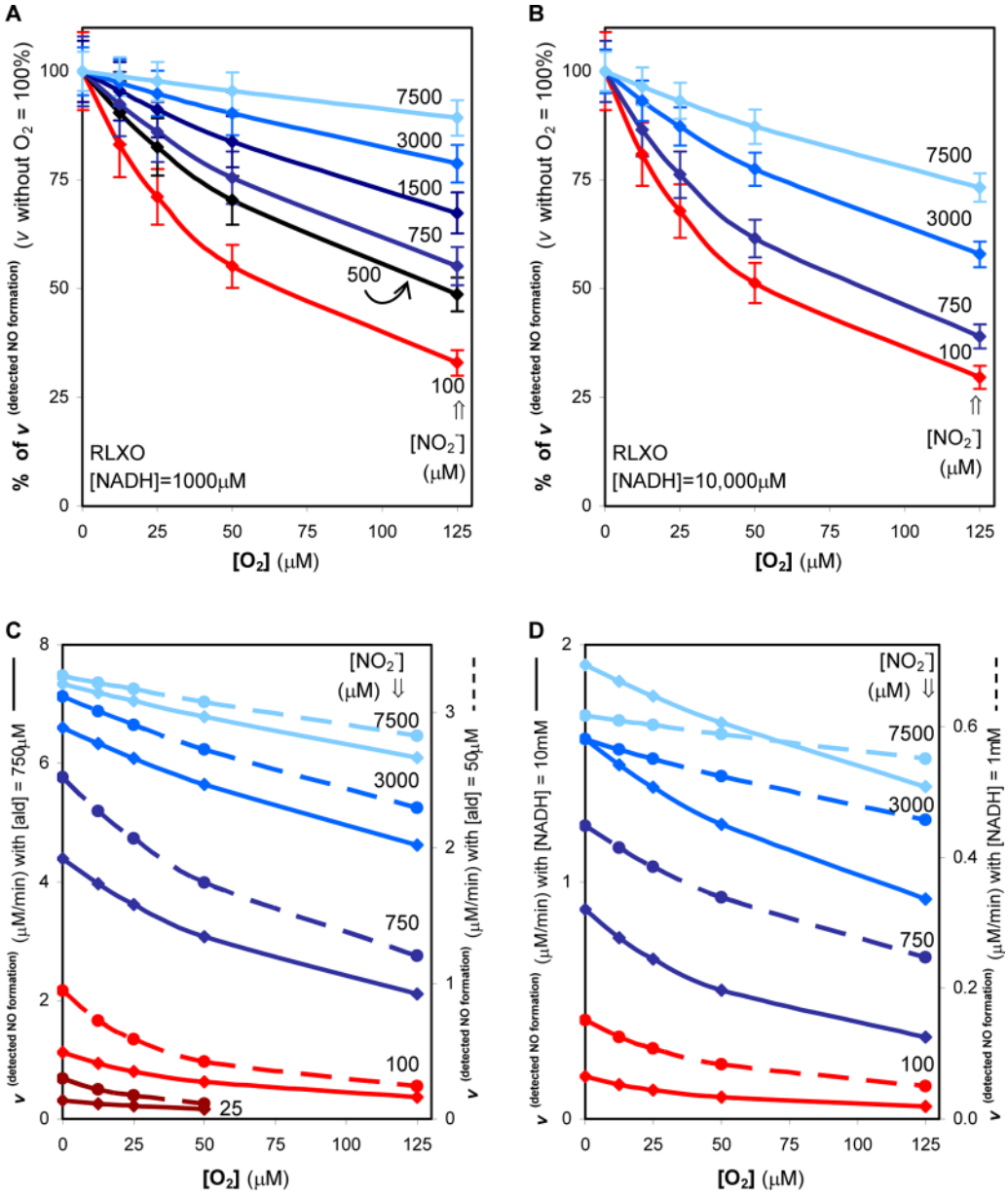

Figure 6. Dioxygen inhibition of RLXO-catalyzed NO formation in the presence of NADH. (A and B) The initial rate of NO formation was measured in the presence of the indicated nitrite, dioxygen, and NADH concentrations with 500 nM RLXO, in the presence of SOD. The NO formation rate observed under anaerobic conditions was taken to be 100% in each case. (C and D) Comparison between aldehyde and NADH. (C) The initial rate of NO formation was measured in the presence of the indicated nitrite, dioxygen, and aldehyde concentrations with 100 nM RLXO, in the presence of SOD. The rates obtained with 750 μM aldehyde are represented with filled lines and refer to the left axis. The rates obtained with 50 μM aldehyde are represented with dashed lines and refer to the right axis. (D) The initial rate of NO formation was measured in the presence of the indicated nitrite, dioxygen, and NADH concentrations with 500 nM RLXO, in the presence of SOD. The rate values determined were divided by 5 to allow for a direct comparison with the aldehyde values that were determined with 5-fold less enzyme. The rates obtained with 10 mM NADH are represented with filled lines and refer to the left axis. The rates obtained with 1 mM NADH are represented with dashed lines and refer to the right axis.

concentrations), the K_i^{app,O_2} data foreshadow $K_i^{O_2}$ values of ≥43 and 49 μM for RLXO and RLAO, respectively.

Effect of Dioxygen on Nitrite Reductase Activity, in the Presence of NADH. The dioxygen inhibition of BMXO-catalyzed NO formation in the presence of NADH has been described to be considerably lower than that observed in the presence of aldehyde or xanthine, with <30% inhibition in the presence of 214 μM dioxygen.[41]

To characterize how the RLXO enzymes behave in this respect, some assays, similar to those described above for aldehyde, but in the presence of NADH, were undertaken (Figure 6A,B). However, because nitrite reduction in the presence of NADH is considerably slower (compared to that of aldehyde), an enzyme concentration that was 5 times higher (500 nM) had to be used, to allow accurate rate measurements.

The dioxygen inhibition observed in the presence of NADH was, in general, lower than that observed in the presence of aldehyde. One potentially relevant exception was observed with 100 μM nitrite, for which similar inhibition values were obtained in the presence of 1000 μM NADH and 750 μM aldehyde. However, we did not observe a marked difference of "NADH versus aldehyde". Relative to that with 750 μM aldehyde (compare

DOI: 10.1021/bi500987w
Biochemistry 2015, 54, 685−710

Figures 5B and 6A), the largest difference of "NADH versus aldehyde" was observed for 1500 μM nitrite and 125 μM dioxygen, where in the presence of aldehyde the inhibition was 40.4 ± 1.7% while in the presence of NADH it was only 33.9 ± 2.3%. Relative to that with 50 μM aldehyde (compare Figures 5A and 6A), the largest difference of "NADH versus aldehyde" was observed for 100 μM nitrite and 50 μM dioxygen, where in the presence of aldehyde the inhibition was 56.0 ± 3.7% while in the presence of NADH it was only 45.3 ± 3.6%. Moreover, our inhibition values were significantly higher than those described by Li et al.[41] For example, 125 μM dioxygen inhibited NO formation from 1000 μM nitrite and NADH by ≈38% [from 2.4 to 1.5 mol min^{-1} (mol of XO)$^{-1}$], while Li et al. described a value of only ≈15% [from 5.2 to 4.4 mol min^{-1} (mol of XO)$^{-1}$].

To assess the influence of the NADH concentration on dioxygen inhibition, some assays were conducted with a very high NADH concentration, aiming to be as close to saturation ($\approx 10K_m^{NADH}$) as experimentally possible (Figure 6B). The NO formation rate for each nitrite concentration increased significantly, compared to that at 1000 μM NADH. However, contrary to what was observed in the presence of a saturating aldehyde concentration, the higher NADH concentration caused an increase in the percentage of dioxygen inhibition at all nitrite concentrations. Nonetheless, once more, the differences of "NADH versus aldehyde" were less than ≈10%.

In summary, although in the presence of NADH the dioxygen inhibition of NO formation was, in general, lower, the inhibition values were similar, within ≈10%, to those obtained with aldehyde (Figure 5 vs Figure 6). Consequently, RLXO-dependent NO formation would not be greatly favored in the presence of NADH, compared to that in the presence of aldehyde. On the contrary, the slower rates of NO formation in the presence of NADH dictate that, in the presence of aldehyde, the level of NO formation should be higher, regardless of the dioxygen inhibition, as can be seen in panels C and D of Figure 6 (where data from Figures 5 and 6A,B are represented not in percentage, but in micromolar per minute).

To have a quantitative measure of the dioxygen inhibition of NADH-dependent NO formation, the K_i^{app,O_2} values were determined. Although the BMXO/NADH/NO_2^-/O_2 system had been described as not displaying saturation kinetics,[41] the RLXO-based system was found to follow Michaelis–Menten kinetics. As was observed with the aldehyde, the k_{cat}^{app,NO_2^-} values do not change significantly with dioxygen concentration, at each NADH concentration. The K_m^{app,NO_2^-} values increased with increasing dioxygen concentrations, being 352, 453, 471, 911, and 1498 μM for 0, 12.5, 25, 50, and 125 μM dioxygen and 1 mM NADH, respectively, and 1117, 1281, 1834, 2576, and 5178 μM for 0, 12.5, 25, 50, and 125 μM dioxygen and 10 mM NADH, respectively. These values resulted in K_i^{app,O_2} values of 32.5 and 34.0 μM for 1 and 10 mM NADH, respectively (Table 2). The similarity between the K_i^{app,O_2} values suggests that those NADH concentrations should be saturating ($>10K_m$) for the reaction of NADH with dioxygen, in the absence of nitrite, which was in fact confirmed (see below and ref 86). At lower concentrations, NADH should modulate dioxygen inhibition. However, the use of lower NADH concentrations requires much higher enzyme concentrations to follow NO formation accurately (because the reaction rate is markedly decreased), which was not viable.

For comparison, and similar to what was done for the system with aldehyde, the K_m^{app,O_2} values for the reaction of NADH with oxygen, in the absence of nitrite, were also determined. For 50 and 500 μM NADH, the K_m^{app,O_2} values were found to be 32.8 and 45.9 μM, respectively (Table 2). These two values suggest that the K_m^{app,O_2} values for 1 and 10 mM NADH should be equal to the real $K_m^{O_2}$, which would be higher, but close to 46 μM. Hence, also in the presence of NADH, the extension of the dioxygen-dependent reactions that can consume the enzymatically generated NO, in the presence of SOD, is relatively small. In addition, the two K_m^{app,O_2} values suggest that the K_m^{NADH} value would be ∼23 μM (considering the only two NADH concentrations to define the straight line of the Hanes plot), confirming that NADH concentrations of 1 and 10 mM are saturating concentrations for the reaction with dioxygen.

Intriguingly, the K_i^{app,O_2} values obtained in the presence of NADH and aldehyde are similar. The two systems, NADH/NO_2^-/O_2 and aldehyde/NO_2^-/O_2, are different from mechanistic and kinetic points of view. The lower dioxygen inhibition observed in the presence of NADH has been attributed to the fact that NADH, while reacting at the FAD center, "blocks" the access of dioxygen to it. This would hinder the dioxygen consumption of electrons derived from the reducing substrate and, consequently, decrease dioxygen inhibition. Simultaneously, the NADH/O_2 reaction is considerably slower [$k_{cat} \geq 0.055$ s^{-1} (Table 2)] than the NADH/NO_2^- reaction [$k_{cat} \geq 0.4$ s^{-1} (Table 2)], which would also favor nitrite reduction over dioxygen reduction. With regard to the aldehyde systems, both aldehyde oxidation and nitrite reduction occur at the molybdenum center, leaving the FAD "free" to react with dioxygen. In addition, the aldehyde/O_2 reaction is faster [$k_{cat} \geq 3.29$ s^{-1} (Table 1)] than the aldehyde/NO_2^- reaction [$k_{cat} = 1.46$ s^{-1} (Table 1)], which would also favor dioxygen reduction. *A priori*, these results would predict that, in the presence of dioxygen, NO formation would be favored in the presence of NADH, compared to aldehyde. However, the two $K_m^{O_2}$ values (for the NADH/O_2 and aldehyde/O_2 reactions) are similar to each other, ≥46 and ≥51 μM, respectively (Tables 1 and 2), and this coincidence is responsible for the similar inhibition constants found here. Moreover, because the specificity for nitrite is much higher in the presence of aldehyde [$K_m^{NO_2^-} = 666$ μM, and $k_{cat} = 1.46$ s^{-1} (Table 1)] than in the presence of NADH [$K_m^{NO_2^-} \geq 1$ mM, and $k_{cat} \geq 0.4$ s^{-1} (Table 2)], NO formation, in the presence and absence of dioxygen, is higher with the aldehyde systems. Finally, also the K_m values for the reducing substrate [$K_m^{ald} = 78.2$ μM, and $K_m^{NADH} \geq 3$ mM (Tables 1 and 2)] suggest that NO formation would be favored in the presence of aldehyde, because lower reducing substrate concentrations would be needed to drive the reaction.

From a physiological point of view, it can be argued that the accumulation of NADH during ischemia[135−138] would drive NADH-dependent NO formation. However, during an ischemic event, undoubtedly other cellular reducing equivalents should accumulate, including hypoxanthine and, subsequently, xanthine.[139−142] Hence, the NO source would be dictated by the enzyme specificity for the different reducing substrates available and by the respective rate of NO formation. In this context, the low RLXO specificity for NADH and the very low rates of NO formation in the presence of physiological NADH concentrations (≪3 mM) suggest that the level of formation of NO from NADH would be rather low, regardless of the inferior dioxygen inhibition, in particular compared to that with hypoxanthine/xanthine.

NO Formation by HepG2 and HMEC. Following the *in vitro* characterization conducted with purified enzymes, it is necessary to demonstrate that XO/XD- and AO-dependent NO formation could, in fact, occur *in vivo* and evaluate its relative

DOI: 10.1021/bi500987w
Biochemistry 2015, 54, 685−710

magnitude and relevance. With that purpose in mind, several studies using differential enzyme inhibition were performed with tissue homogenates, namely, heart, aorta, and liver,[41,42] and with animal models of myocardial infarction,[21] renal,[23] cardiac,[18] and liver[20] ischemia/reperfusion injury, etc.[19,25,27−31] Various approaches have been developed to measure NO formation in biological samples, but most of them detect NO only after it has diffused out of the cell or tissue or after cell disruption (such as chemiluminescence that measures NO in the gas phase or the spin-traps/EPR and NO-specific electrodes used here). To overcome this limitation and measure NO formation inside a living cell, a microelectrode or a nontoxic cell-permeable probe must be used.

In this work, the physiological relative relevance of XO/XD and AO to the NO formation was evaluated with a fluorescence probe, using two cell lines, HepG2 and HMEC, subjected to hypoxia, in 23 and 43 μM dioxygen, to mimic the conditions characteristic of ischemia. NO formation inside living cells was followed with the DAF-FM DA (DAF-FM diacetate) probe. DAF-FM DA is a nonfluorescent, cell-permeant compound that passively diffuses across the cell membrane; inside cells, it is deacetylated by intracellular esterases to yield DAF-FM. Once the acetate groups are removed, the two aromatic vicinal amine groups of DAF-FM react (indirectly) with NO to form a highly fluorescent triazole product.[143,144] However, the mechanism behind the fluorophore formation is complex, because diaminofluoresceins do not react with NO itself, but with an active intermediate formed in the course of the reaction of NO with dioxygen, suggested to be the dinitrogen trioxide (eq 8 → eq 9).[143,144] Hence, the rate at which NO is oxidized to dinitrogen trioxide imposes an intrinsic limitation on detection by this method and introduces a significant variability within assays conducted under different conditions.[143,144]

To validate the fluorimetric method, NO formation was followed in a simplified system, using purified BMXO (no cells), with the DAF-FM[d] probe, under 20 μM dioxygen (Figure 7). At pH 5.0, the fraction of BMXO-independent NO detected is considerable (Figure 7, first group of striped bars), in particular in the presence of 240 μM nitrite, when both BMXO-independent (striped red bar) and BMXO-dependent (filled red bar) NO formation rates are similar. In contrast, at pH 6.0, only BMXO-dependent NO generation is detected (Figure 7, last group of bars).

Protein-independent NO formation relies on the decomposition of nitrite to dinitrogen trioxide at acidic pH (eq 11 → eq 12); dinitrogen trioxide can then dismutate to NO and nitrogen dioxide radical (eq 9′).[145−148] The extent of the protein-independent NO generation is expected to be comparatively small and limited to conditions of extreme acidosis, because it depends on (i) the formation of nitrous acid (eq 11; $pK_a = 3.2$) and (ii) the dismutation of dinitrogen trioxide, whose equilibrium (eq 9′) is rapidly dislocated toward NO consumption ($k \approx 10^9$ M^{-1} s^{-1}), instead of NO formation ($k \approx 10^4$ s^{-1}).[33,145,148] Nevertheless, the rate and direction at which reactions 11 → 12 → 9′ would be driven (either *in vitro* or *in vivo*) depend not only on the pH but also on (i) the presence of reducing compounds (such as traces of transition metals present in solutions) and (ii) factors that shift the equilibria by consuming NO (such as dioxygen, or DAF-FM that consumes dinitrogen trioxide).[149]

$$2NO_2^- + 2H^+ \rightleftharpoons 2HNO_2 \quad (11)$$

$$2HNO_2 \rightleftharpoons H_2O + N_2O_3 \quad (12)$$

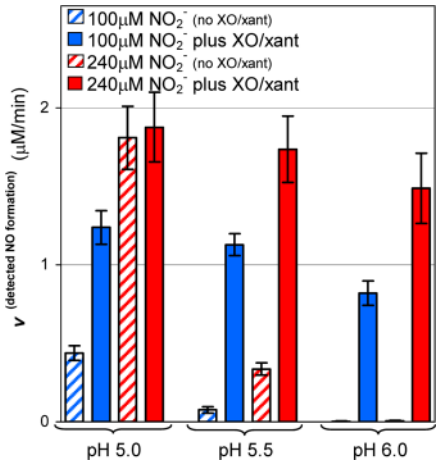

Figure 7. BMXO-catalyzed NO formation evaluated by fluorescence spectroscopy with the DAF-FM probe. The rate of NO formation was measured (i) in the presence of 100 and 240 μM nitrite and in the absence of BMXO and xanthine (striped blue and red bars, respectively) and (ii) in the presence of 100 and 240 μM nitrite with 65 milliunits/mL BMXO and 50 μM xanthine (filled blue and red bars, respectively). The rate observed in the absence of BMXO and xanthine corresponds to BMXO-independent NO formation. These values were subtracted from the rate in the presence of BMXO and xanthine for the respective nitrite concentration. Therefore, the values represented as filled bars correspond to only BMXO-dependent NO formation. NO formation was followed at the pH values indicated, in the presence of 20 μM dioxygen, 10 μM DAF-FM, and 600 units/mL SOD, as described in Experimental Procedures.

$$N_2O_3 \rightleftharpoons {}^{\bullet}NO + {}^{\bullet}NO_2 \quad (9')$$

Therefore, we suggest that, at low pH values, several reactions occur simultaneously in the fluorescence assays. On one hand, nitrite is reduced to NO by BMXO, in a reaction that would increase as the pH is increased from 5 to 6 (Figure 3). The detection of this NO is limited by the rate at which NO is oxidized to dinitrogen trioxide. On the other hand, nitrite is converted into dinitrogen trioxide, in a protein-independent manner (eq 11 → eq 12). The dinitrogen trioxide thus formed can react with DAF-FM, dismutate to form NO (eq 9′), or be hydrolyzed (eq 10; $k \approx 10^3$ s^{-1}). On the basis of the equilibrium constant of reaction 10′ (10^{-5} M) and the high probe concentration present (10 μM), we suggest that the majority of dinitrogen trioxide would not be converted into NO; on the contrary, it would react directly with DAF-FM without being ever converted into NO, though a dinitrogen trioxide fraction could be converted into NO, as described by others.[123,124] Therefore, "NO formation" that does not reflect true NO formation could be observed (i.e., a fluorescent signal could be detected). The detection of this "NO-like" signal would be limited mainly by pH (that controls reactions 12 and 13). Hence, as the pH is increased from 5 to 6, the fraction of conversion of protein-independent nitrite into dinitrogen trioxide is decreased, while the fraction of XO-dependent NO formation is increased. It is the outcome of these two pathways, which follow opposite pH profiles, that gives rise to the pH profile in Figure 7. Moreover, as the pH is increased toward 6.0, XO-dependent NO formation becomes clearly dominant (Figure 7, last group of bars), as is observed in the assays with the NO electrode or by EPR spectroscopy (Figure 1). Because the results from this simplified study could be reasonably explained, we employed this fluorescence method to evaluate NO formation by the cell lines.

DOI: 10.1021/bi500987w
Biochemistry 2015, 54, 685−710

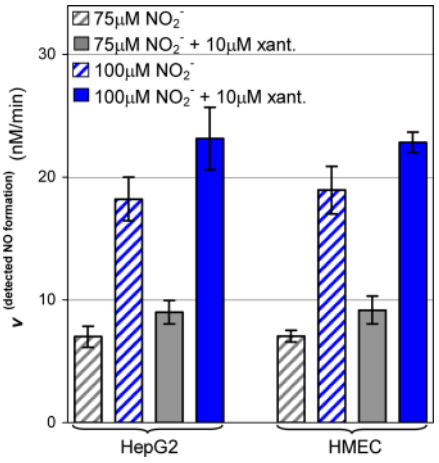

Figure 8. Nitrite-dependent NO formation by HepG2 and HMEC. Intracellular NO formation by HepG2 and HMEC was followed in the presence of 75 and 100 μM nitrite (gray and blue bars, respectively), with 23 μM dioxygen, at pH 5.5. NO formation was followed in cells to which only nitrite was added (striped bars) and in cells to which nitrite and 10 μM xanthine were added (filled bars). NO formation was followed in the presence of 10 μM DAF-FM DA, as described in Experimental Procedures.

Both HepG2 and HMEC elicited nitrite-dependent NO formation to similar extents and in a pH-dependent manner. In both cell types, NO generation was found to decrease as the pH increases from 5.0 to 5.5, being even lower at pH 6.0. Because the fraction of protein-independent conversion of nitrite into dinitrogen trioxide at pH 5 is expected to be high [as was observed with purified BMXO (Figure 7)], we focused our studies with the cells on pH 5.5.

Nitrite concentrations of 75 and 100 μM triggered considerable NO formation, 7.01 ± 0.85 and 18.2 ± 1.76 nM/min in HepG2 and 7.05 ± 0.47 and 19.0 ± 0.32 nM/min in HMEC, respectively (Figure 8), thus approaching the order of magnitude of the NO formation rate by constitutive NOS (≈60 nM/min).[9]

The observed NO formation is clearly nitrite-dependent, because increasing nitrite concentrations resulted in an increase in the NO formation rate. The absence of an effect of L-NAME, a specific NOS inhibitor, confirmed that NO generation observed was independent of NOS and totally dependent on nitrite. To highlight the relevance of reducing substrates to enzymatic NO formation, some assays were conducted in the presence of 10 μM xanthine (Figure 8, full bars). The addition of xanthine caused a 15−36% increase in NO generation, suggesting that XO is contributing to NO formation and that the reducing substrate availability might limit enzymatic nitrite-dependent NO formation.

To evaluate the relative contribution of XO and AO to the observed NO formation, the effect of specific inhibitors was explored (Figure 9A). While the presence of rotenone, a mitochondrial complex I inhibitor, caused no effect, allopurinol and raloxifene, XO- and AO-specific inhibitors, respectively, do inhibit the NO generation of cells. Allopurinol inhibited NO formation in HepG2 and HMEC by 29.5 ± 6.1 and 30.3 ± 4.7%, respectively, while raloxifene caused a lower inhibition of 23.4 ± 10.2 and 16.8 ± 4.7%, respectively. Of note, this XO versus AO relation is in agreement with the comparison made taking into account the real kinetic parameters at pH 6.3 (Table 1) that predicted that the contribution of AO to NO formation would be lower than that of XO. The inhibition effect was additive, as expected if two independent enzymes are generating NO simultaneously, and in the presence of both inhibitors, NO formation by HepG2 and HMEC decreased by 50.1 ± 9.4 and 50.5 ± 2.9%, respectively. It is noteworthy that the contributions of XO and AO to NO formation in other systems are on the same order of magnitude. For example, in rat heart homogenates, with 2% dioxygen, oxypurinol was shown to inhibit NO formation by >60%[41] and oxypurinol and raloxifene inhibited anaerobic NO formation by rat liver and heart homogenates by 76 and 66%, respectively.[42]

The effect of dioxygen on NO formation by cells was also studied. Under normoxia, the tissue dioxygen concentration is ∼50 μM,[134] and during mild hypoxia, it can decrease to

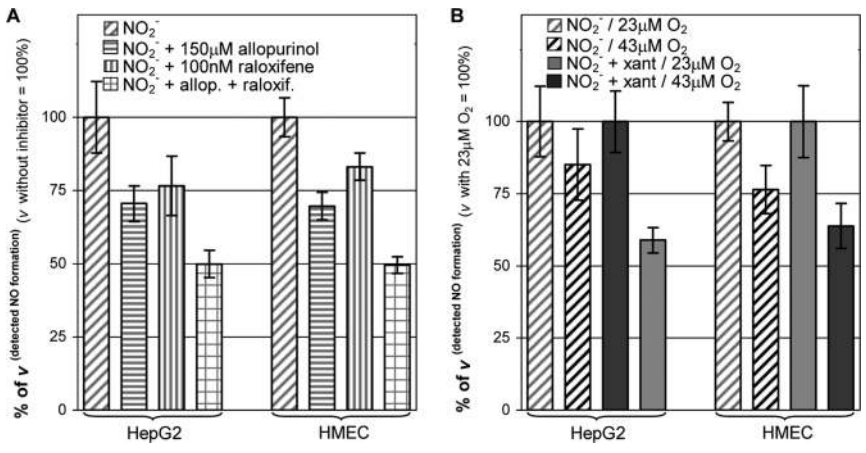

Figure 9. Effect of XO- and AO-specific inhibitors (A) and dioxygen inhibition (B) on nitrite-dependent NO formation by HepG2 and HMEC. (A) The intracellular NO formation by HepG2 and HMEC was followed with 75 μM nitrite in the absence of inhibitors (diagonally striped bars) and in the presence of 150 μM allopurinol (horizontally striped bars), 100 nM raloxifene (vertically striped bars), and both allopurinol and raloxifene (squared bars), with 23 μM dioxygen. For each cell type, the NO formation rate observed in the absence of inhibitors was taken to be 100% (the respective values in nanomolar per minute are represented in Figure 8). (B) The intracellular NO formation by HepG2 and HMEC was followed in the presence of 75 μM nitrite, with 23 and 43 μM dioxygen (striped gray and dark gray bars, respectively). NO formation was also followed in the presence of 75 μM nitrite and 10 μM xanthine (filled gray and dark gray bars for 23 and 43 μM dioxygen, respectively). In each case, the NO formation rate observed with 23 μM dioxygen was taken to be 100% (the respective values in in nanomolar per minute are represented in Figure 8). NO formation was followed in the presence of 10 μM DAF-FM DA, as described in Experimental Procedures.

DOI: 10.1021/bi500987w
Biochemistry 2015, 54, 685−710

10−30 μM.[124,150] Hence, two dioxygen concentrations were studied, one typical of hypoxia, 23 μM, and another close to normoxia, 43 μM. As expected from the *in vitro* studies (Figures 4 and 5), dioxygen decreased NO formation (Figure 9B). However, the dioxygen increase from 23 to 43 μM caused only a relatively small decrease of 14−23% (Figure 9B, striped gray and dark gray bars). These results demonstrate that even at a relatively high dioxygen concentration (close to normoxia), nitrite-dependent NO formation is still observed, which supports the reasonability and feasibility of this NO formation pathway. Interestingly, dioxygen inhibition in the presence of added xanthine was higher, 32−41% (Figure 9B, filled gray and dark gray bars). This result further corroborates the fact that XO is contributing to NO formation and that the availability of the cellular reducing substrate (at least to XO) might be limiting enzymatic nitrite-dependent NO formation.

DISCUSSION

***In Vitro* Characterization of Rat and Human Liver XO/XD and AO Nitrite Reductase Activity.** The reduction of nitrite to NO by XO and AO, from rat and human liver, is dependent on the presence of three components, nitrite, a reducing substrate, and an enzyme (Figure 1). No NO formation is observed in the absence of any of those three reactants, demonstrating clearly that nitrite reduction or NO formation by rat and human liver enzymes is an intrinsic property of the enzymes. Moreover, nitrite reduction is independent of the nature of the reducing substrate and of its site of reaction: NO generation is triggered by both aldehydes (DHB and DMAC) and heterocyclic compounds (xanthine and NMN) that react at the molybdenum center and NADH that reacts at the FAD center.

For the first time, the nitrite reductase activity of a XD enzyme was characterized (Figures 1−3 and Table 1) and it was confirmed that RLXD displays kinetic parameters similar to those of RLXO. The two enzymatic forms, XO and XD, are known to differ only on the structure around the FAD center, showing no significant differences in terms of the global folding at the Fe/S and molybdenum centers or the kinetics of reactions occurring at the molybdenum center.[62,76,77] Although the similarity between XO and XD was expected, the necessary confirmation had not yet been made.

Also for the first time, the nitrite reductase activity of true human XO and AO was characterized (Figures 1−3 and Table 1). The similarities found in the kinetic parameters, at pH 7.4 and 6.3, of human liver and rat liver enzymes are of major importance. It supports the employment of rat liver enzymes (whose tissue is easier to obtain in large amounts) as suitable models of the human counterparts, while an appropriate recombinant expression system for fully functional human enzymes is not available. A full kinetic characterization of both human enzymes was not feasible, but the results obtained with the rat liver enzymes can be, in this way, extrapolated with some confidence to be applied to the human enzymes.

It is noteworthy that the specificity of the enzymes for nitrite was found to increase significantly, ≈8 times, when the pH is lowered from 7.4 to 6.3, being 2.19 and 1.64 × 10^3 M^{-1} s^{-1} at pH 6.3 for RLXO and RLAO, respectively (Table 1). This finding is of major importance for the potential *in vivo* role of XO/AO-dependent NO generation under ischemia, when the pH can decrease to values as low as 6.0−5.5 (acidosis).[119−124] With regard to the comparison of RLXO versus RLAO, at pH 6.3, although the limiting rate of AO reaction is higher (3.37 s^{-1} vs 1.46 s^{-1}, respectively), its superior $K_m^{NO_2^-}$ value (2.05 mM vs 666 μM, respectively, resulting in the lower specificity for nitrite) suggests that the relative contribution of AO to NO generation would be smaller than that of XO.

Furthermore, the comprehensive kinetic characterization of the effect of pH on XO- and AO-catalyzed nitrite reduction (Figure 3 and Table 1) allowed three key conclusions to be reached. (i) The specificity constants for nitrite/pseudo-first-order rate constants exhibited a bell-shaped pH curve, with maximal values at pH ≈6.3−6.5, which correspond to an ≈8-fold increase, relative to that at pH 7.4. (ii) The k_{cat}^{app,NO_2^-} curves followed the same pH profile, indicating also that the highest rates of NO formation occur at pH values between 5.8 and 6.8 (1.19−1.32 and 1.90−3.00 s^{-1} for XO and AO, respectively). (iii) The K_m^{app,NO_2^-} values displayed an inverted bell-shaped pH curve, decreasing significantly, ≈5−6-fold, at pH ≤6.8 (relative to that at pH 7.4) with minima of 603 μM and 1.83 mM for XO and AO, respectively. As a result, at pH 5.8−6.8, the pseudo-first-order rate constants reach their maximal values and the $K_m^{NO_2^-}$ values are minimized. The simultaneous occurrence of these two results is particularly relevant. (i) The pseudo-first-order rate constant refers to the reaction rate when nitrite is present at a concentration much lower than its $K_m^{NO_2^-}$. Because the *in vivo* nitrite concentration (<20 μM[125−128]) is also much lower than the $K_m^{NO_2^-}$, it is significant that the highest pseudo-first-order rate constants are attained at acidic pH values characteristic of ischemia, precisely when a nitrite-dependent, NOS-independent, NO source would be needed. This pseudo-first-order rate constant pH dependence allows the enzymes to overcome the constraint imposed by the high $K_m^{NO_2^-}$ values and low nitrite availability. (ii) Concomitantly, also the decrease in $K_m^{NO_2^-}$ would contribute to the potential *in vivo* NO formation, because lower nitrite concentrations would be needed to drive a similar reaction rate of NO generation. Moreover, the XO $K_m^{NO_2^-}$ value on the order of millimolar is one of the strongest arguments raised against its involvement in *in vivo* NO formation. The comprehensive kinetic characterization presented here shows that the discrepancy between $K_m^{NO_2^-}$ and the *in vivo* nitrite concentration is pH-dependent, being minimized under acidic conditions and not being as high as previously envisaged [i.e., K_m^{app,NO_2^-} values of ≈600 μM (pH 6.3) and not ≈3 mM (pH 7.4)].

Because dioxygen should interfere with the status of NO (Scheme 2), its effects were also studied at pH 6.3. Dioxygen is able to decrease the amount of XO/AO-dependent NO formed (both *in vitro* and *in vivo*) and also the amount of NO available to be detected (*in vitro*) or to exert its physiological functions (*in vivo*). The comprehensive study allowed the following major conclusions to be reached. (i) Under our assay conditions, and because we considered only initial rates, the direct reaction of NO with dioxygen (eq 8) can be neglected [considered to be within the experimental error (Figure 4A)]. (ii) On the other hand, NO consumption by superoxide radical (eq 6) in the absence of SOD is substantial, regardless of the dioxygen concentration present (Figure 4B). This "NO sink" is particularly relevant when the nitrite concentration is limiting, because the competition between nitrite and dioxygen is unfavorable to nitrite and more superoxide is formed. These results highlight the physiological relevance of SOD in achieving net NO production. (iii) In addition, dioxygen is also a strong competitive inhibitor of XO- and AO-dependent NO formation (eq 5, Figure 5, and Table 1), because it efficiently consumes the electrons of the enzymes needed to reduce nitrite (eq 1). Nevertheless, and remarkably, it is possible to detect NO formation from only

DOI: 10.1021/bi500987w
Biochemistry 2015, 54, 685−710

25 μM nitrite, in the presence of dioxygen concentrations as high as 50 μM, that is, at the normal (normoxic) tissue dioxygen concentrations.[134] With 100 nM RLXO, under those conditions, the NO formation rates are 121 ± 21 and 166 ± 19 nM/min with 50 and 750 μM aldehyde, respectively, and correspond to dioxygen inhibitions of ≈60 and ≈50%, respectively.

To quantify dioxygen inhibition, the K_i^{app,O_2} values were determined and found to be 24.3 and 42.7 μM for RLXO and 50 and 750 μM aldehyde, respectively, and 25.2 and 48.8 μM for RLAO and 50 and 1500 μM aldehyde, respectively (Table 1). It is noteworthy that these K_i^{app,O_2} values are within the range of *in vivo* tissue dioxygen concentrations (≤50 μM, going from normoxia to hypoxia[134]), which suggests that *in vivo* NO formation could be fine-tuned by dioxygen availability. Moreover, these results demonstrate that the aldehyde concentration present does have a marked effect on the K_i^{app,O_2} value, suggesting also that the *in vivo* available reducing substrate concentration could control NO formation through modulation of dioxygen inhibition. Hence, the accumulation of ischemia-induced reducing substrates could create enzyme saturating conditions, which would favor nitrite reduction and also lead to lower dioxygen inhibitions.

Dioxygen inhibition was also studied in the presence of NADH (Figure 6 and Table 2). The K_i^{app,O_2} values obtained were similar to those given above, being 32.5 and 34.0 μM for 1 and 10 mM NADH, respectively. In this case, the reducing substrate modulation of the dioxygen inhibition was not observed (both K_i^{app,O_2} values are identical), because the NADH concentrations used are saturating ($\gg 10K_m^{NADH}$) for the reaction of NADH with dioxygen, in the absence of nitrite. At lower concentrations, NADH should modulate dioxygen inhibition, as observed with the aldehyde. With regard tog the comparison between NADH and aldehyde, although in the presence of NADH dioxygen inhibition of NO formation was, in general, lower, the inhibition values were similar to (within ≈10% of) those obtained with aldehyde, as expected from the similarity in the K_i^{app,O_2} values. Accordingly, RLXO-dependent NO formation would not be greatly favored in the presence of NADH, compared to that in the presence of the aldehyde. On the contrary, the slower rates of NO formation in the presence of NADH dictate that, in the presence of aldehyde, NO formation should be higher, regardless of the superior dioxygen inhibition (Figure 6C,D). From a physiological point of view, during an ischemic event, the NO source would be dictated by the specificity of the enzyme for the different reducing substrates available, their concentration, and the respective rate of NO formation. Although the NADH concentration would increase, the comparatively low RLXO specificity for NADH ($k_{cat} \geq 0.4\ s^{-1}$, and $K_m^{NO_2^-} \geq 1$ mM) and the very low rates of NO formation in the presence of physiological NADH concentrations ($\ll 3$ mM $\leq K_m^{NADH}$) suggest that NO formation from NADH would be rather low, regardless of the inferior dioxygen inhibition, in particular compared to that of hypoxanthine/xanthine (that would also accumulate).

Overall, our *in vitro* studies provide relevant information about the nitrite reductase/NO synthase activity of mammalian liver XO/XD and AO. XO/XD/AO-dependent NO formation would be modulated by several factors. (i) Availability of reducing substrates. First, and obviously, because they provide the electrons needed to reduce nitrite but also because we have shown that their concentration would determine the extension of dioxygen inhibition. (ii) pH. Although previous discrete (single-nitrite concentration) basic kinetic assays have suggested that NO formation would be favored at acidic pH values, in this work we quantified the effects of pH on the k_{cat} and K_m parameters and clearly demonstrated that nitrite reduction by both enzymes is greatly favored under acidic conditions (pH <6.8). (iii) Dioxygen concentration. We have shown that the $K_i^{O_2}$ values are within the range of physiological dioxygen concentrations and suggested that the dioxygen availability would fine-tune NO formation and not completely abolish NO generation. (iv) SOD. Our results further emphasized the physiological relevance of SOD in achieving net NO production under nonanoxic conditions, because the superoxide radical formed by XO/XD/AO in the presence of dioxygen rapidly scavenges the NO formed. (v) Nitrite availability, of course. Hence, during an ischemic event, the resulting acidosis that reduces the accumulation of substrates and the limited dioxygen availability or its absence could trigger the XO/XD/AO-dependent NO formation if nitrite is available and SOD is locally present.

Reaction Mechanism for Liver XO/XD and AO Nitrite Reductase Activity. Previous work and this work have demonstrated unequivocally that nitrite reduction takes place at the enzyme's molybdenum center (see Enzyme Redox Center Responsible for Nitrite Reduction and NO Formation). Moreover, the NO formed during the catalytic cycle is not able to significantly react with the molybdenum sulfo group (Scheme 1, i) and inhibit the enzymes.

On the basis of kinetic and EPR spectroscopic data, we have proposed the first molecular mechanism of nitrite reduction.[43] This kinetic characterization of the effect of pH on nitrite reductase activity allowed us to further refine the suggested mechanism.

To catalyze the reduction of nitrite to NO, an enzyme has to bind nitrite, transfer one electron to it, cleave a N−O bond, abstract one of the nitrite oxygen atoms, and, ultimately, release the NO formed. In XO/XD and AO, we suggest that the reaction occurs as follows.

During the first part of the catalytic cycle (oxidation half-reaction), molybdenum is reduced by a reducing substrate (e.g., aldehyde; briefly described in footnote [e]). Subsequently, nitrite binds to it, displacing the bound product (carboxylate) through the formation of a ternary "carboxylate−Mo^{4+}−nitrite" complex, as suggested for BMXO,[43] or displacing a water molecule, as the "ping-pong" kinetic mechanism type of RLXO and RLAO described herein suggests. We did not find any spectroscopic evidence of interaction of nitrite with oxidized molybdenum, and NO formation occurs only after molybdenum reduction;[43] therefore, nitrite is proposed to bind only to reduced molybdenum. Furthermore, nitrite is suggested to be bound to the molybdenum atom through one of its oxygen atoms ["nitrito" binding mode (Scheme 1, ii, d)], as is observed in other substrates and/or product complexes of XO family enzymes (that also interact through an oxygen atom).[58−64] The chemistry of Mo^{6+}, Mo^{5+}, and Mo^{4+} is dominated by the formation of oxides and sulfides, but the strong tendency of molybdenum to bind oxo groups is balanced by its ability to easily lose a single oxygen atom.[153] This chemistry makes the molybdenum cores excellent "oxygen atom exchangers", as long as the thermodynamics of the reactions is favorable,[154] precisely what is needed to convert nitrite into NO.

Subsequently, one electron is transferred from molybdenum to nitrite. In this step, molybdenum is oxidized to Mo^{5+} (giving rise to the characteristic rapid type 1 EPR signal) and, simultaneously, NO is formed (as evaluated with the selective electrode and by EPR spectroscopy)[43] (Scheme 1, ii, e → f).

DOI: 10.1021/bi500987w
Biochemistry 2015, 54, 685−710

To accomplish this, the molybdenum center has to promote N−O bond cleavage (O−N−O → N═O) and release the NO formed. We suggest that this step (Scheme 1, ii, e → f) is triggered by a protonation event. As discussed above (in Effect of pH on Nitrite Reductase Activity), nitrite reduction or NO formation is greatly favored at pH <6.8 and involves two protonation equilibria, with pK_a values of 5.9 and 6.8 (XO) and 6.0 and 7.0 (AO). The identity of the ionizable groups responsible for those pK_a values is difficult to anticipate in light of our knowledge of the XO active site pocket and mechanism of reaction. However, the bell-shaped pH curves of $k^{NO_2^-}$ (Figure 3) may also arise from a single ionizable group that is required in different states in two steps of the catalytic cycle (Scheme S1 of the Supporting Information), and we suggest that such a group is the conserved key glutamate residue (BMXO Glu_{1261}). Accordingly, we propose that (i) in the first part of the catalytic cycle [oxidation half-reaction (Scheme 1, ii, a → b)], the deprotonated glutamate functions as a base and assists the nucleophilic attack of Mo−O^- on the carbon center to be hydroxylated and (ii) during the nitrite reduction part (reduction half-reaction), the same glutamate residue, but at this point protonated, functions as the proton donor required to reduce nitrite (eq 1 and Scheme 1, ii, e → f).

The hypothesis raised here that the conserved key glutamate residue participates in the catalytic cycle in two different protonation states is reasonable. (i) At present, it is clear that, while the hydroxylation of xanthine or aldehyde is favored at higher pH values (>7[129,130]), nitrite reduction requires more acidic conditions (<7). Thus, the global catalytic cycle has a dual pH dependence. (ii) In this scenario, this glutamate residue has the adequate and best position inside the active site pocket to act as the proton donor (Scheme 1, i).

Hence, we suggest that, once the Mo^{4+}−O−N−O complex is formed (Scheme 1, ii, d), the reaction proceeds with protonation of the nitrite oxygen atom bound to the molybdenum, at the expense of the glutamate residue (Scheme 1, ii, e). This protonation step could trigger the transfer of an electron from the reduced molybdenum to the now protonated nitrite, causing N−OH bond homolysis and subsequent NO release. Furthermore, the previous protonation of nitrite (Scheme 1, ii, e) would lead to the formation of a more stable "future" metal complex; that is, it would lead to the formation of a Mo^{5+}−OH complex (Scheme 1, ii, f) instead of a Mo^{5+}−O^- complex. The pK_a values of the molybdenum-coordinated ligands change dramatically with the oxidation state, and the lower oxidation states hold highly protonated ligands.[155,156] For this reason, in the Mo^{5+} complex (Scheme 1, ii, f), both terminal oxygen and sulfur atoms should end up protonated (this complex would produce the characteristic Mo^{5+} rapid-type EPR signal, with two interacting protons). If nitrite is protonated before it is converted into NO, the "future" metal complex would end up in a more stable form [Mo^{5+}−OH (Scheme 1, ii, f)].

A similar mechanism was proposed for the reduction of nitrite to NO by bacterial copper-containing nitrite reductase (CuNiR). This enzyme displays a similar pH dependence, with pK_a values of 5 and 7, and theoretical calculations have suggested that it is the proton transfer from a key aspartate residue (pK_a of 5) that triggers the electron transfer from copper to nitrite (proton transfer triggering electron transfer).[157] Moreover, also in CuNiR, the previous nitrite protonation results in the formation of a more stable metal complex, Cu−OH instead of Cu−O^-.

The mechanism by which XO/XD and AO promote N−OH bond cleavage is presently not known. However, it is tempting to speculate that the strategy followed by the molybdoenzymes would be analogous to that of CuNiR,[f] because both metals share the same square pyramidal geometry and have a redox active HOMO on the $x-y$ plane (d_{xy} and $d_{x^2-y^2}$ for molybdenum and copper, respectively).[158−160]

At this stage (Scheme 1, ii, f), one molecule of NO is already formed and released. However, because xanthine and aldehyde oxidation is a two-electron process (Mo^{6+} → Mo^{4+}), another nitrite molecule could be reduced. Thus, the reaction is proposed to proceed with the binding of a second nitrite molecule. To generate a good leaving group, water (Mo^{5+}−OH_2), the consumption of one proton is suggested (Scheme 1, ii, f → g). Subsequently, nitrite displaces the water molecule (Scheme 1, ii, g → h), and after a second cycle of nitrite reduction and molybdenum oxidation, a second NO molecule is released (Scheme 1, ii, h → a). The molybdenum is now in a 6+ oxidation state (Scheme 1, ii, a), which would favor the deprotonation of its ligands[155,156] and make it ready to start a new catalytic cycle.

In summary, XO/XD- and AO-catalyzed nitrite reduction is suggested to be initiated with the nitrite binding to the reduced molybdenum center, in a "nitrito" binding mode (i.e., through one oxygen atom). After a protonation event, hypothesized to be mediated by the conserved glutamate residue, the electron transfer from molybdenum to nitrite is triggered, the N−OH bond homolytically cleaved, and the NO promptly released. The proposed mechanism is presently being thoroughly examined by theoretical calculations.

The unique molybdenum chemistry makes the molybdenum centers excellent "oxygen atom exchangers", and molybdoenzymes are widely used to catalyze oxo transfer reactions, both oxo abstractions and oxo insertions, in the metabolism of carbon, sulfur, and nitrogen.[58−64,161−164] In this context, it is surprising that no "dedicated" molybdenum-containing nitrite reductase is known to exist. This reasoning makes us think that it is probable that living organisms are using molybdenum to synthesize NO but employing enzymes that we attribute to other functions. Mammalian XO/XD, AO, sulfite oxidase, mitochondrial amidoxime reducing component, plant nitrate reductase, and bacterial aldehyde oxidoreductase and nitrate reductases may become the first examples of such utilization to be described.[33,34]

Human XO/XD and AO Nitrite Reductase Activity: NO Formation by HepG2 and HMEC. The potential relative physiological relevance of XO/XD and AO to NO formation was herein evaluated using two cell lines, HepG2 and HMEC, subjected to hypoxia, 23 and 43 μM dioxygen, to mimic the conditions characteristic of ischemia. Both HepG2 and HMEC generate nitrite-dependent NO, to similar extents and in pH-dependent manners (Figure 8). As the pH is increased, the fraction of protein-independent nitrite conversion decreases and the fraction of XO/XD/AO-dependent nitrite reduction to NO increases, accounting for ≈50% of NO generation at pH 5.5 (Figure 9A). NOS and mitochondrial complex I do not contribute to the observed NO generation (no L-NAME or rotenone inhibition). In addition, cellular NO formation is clearly nitrite-dependent and might be limited by the availability of XO/XD/AO reducing substrates in HepG2 and HMEC (Figure 8). Most importantly, although dioxygen decreases the observed NO generation, the observed diminution was small [14−23%, for a dioxygen increase from 23 to 43 μM (Figure 9B)] and considerable NO formation was still observed even at a dioxygen concentration close to normoxia (43 μM). Hence, nitrite-dependent XO/XD/AO-catalyzed NO generation can occur

DOI: 10.1021/bi500987w
Biochemistry 2015, 54, 685−710

inside living cells under hypoxia and, to a minor extent, under normoxia.

The characterization of NO generation by cell lines is by far more complex than the *in vitro* studies. Cells, themselves, are complex, and several pathways can contribute to the generation of NO and "NO-like" compounds.[33,34] In addition, NO and "NO-like" compounds are dynamic metabolites that react with a myriad of cellular components, mostly heme-containing proteins, labile [4Fe-4S] centers, cysteine residues and other thiols, and reactive oxygen species.[2,6−9] These physiological reactions would compete with the reaction with the fluorescence probe, and an important fraction of NO can escape detection. Also, the rate at which NO is oxidized to dinitrogen trioxide inside the cells would modulate NO detection. Nevertheless, the use of a cell-permeable fluorescence probe allows NO detection to be much closer, in space and time, to the sites of NO production and consumption and, thus, provide a more consistent evaluation of NO metabolism.

Overall, our results with HepG2 and HMEC support the feasibility and reasonability of human nitrite-dependent XO/XD/AO-catalyzed NO formation. The NO metabolic fluxes through these pathways would be modulated by the availability of nitrite, dioxygen, and reducing substrates and by the presence of SOD.

This demonstration of XO/XD/AO-dependent nitrite-derived NO generation by HepG2 and HMEC came in line with several other studies performed with tissues homogenates (heart, aorta, and liver),[41,42] models of myocardial infarction,[21] renal,[23] cardiac,[18] and liver[20] ischemia/reperfusion injury, pulmonary arterial hypertension,[26−28] etc.[19,25,29] Together, all these studies provide consistent support for the participation of XO/XD and AO in NO generation pathways. Nevertheless, this is a controversial subject, and conflicting results have being described. For example, while Webb and colleagues reported that XO from erythrocytes[25,30] and blood vessels[25] contributes to the generation of intravascular vasodilator NO, Dejam et al.[22] found in humans that infusions of oxypurinol do not inhibit nitrite-dependent vasodilation (on the contrary, they potentiate it), thus excluding the involvement of XO. In addition, a recent study showed that oxypurinol does not have any effect on the nitrite-dependent inhibition of platelet reactivity.[32] Clearly, although the understanding of nitrite physiological roles has evolved considerably over the last two decades, there still are numerous open questions to be answered. Our results aim to contribute to the debate.

CONCLUSION

Human NO is a key signaling molecule that is involved in numerous physiological processes and also in some pathological conditions. At present, it is clear that NO can be formed by two distinct pathways, which operate under opposite conditions: (i) an oxidative pathway, which is mediated by specific NOS enzymes and depends on dioxygen, (ii) and a reductive pathway, which is mediated by "nondedicated" nitrite reductases, depends on nitrite, and is favored at low dioxygen concentrations and under acidic conditions. With these two pathways, cells can maintain vital NO formation over the entire oxygen gradient, from normoxia to anoxia.

The knowledge of nitrite physiological roles in mammals has evolved considerably over the past two decades, giving a novel relevance to this formerly "useless" end product of NO metabolism.[33,34] The "simple" one-electron reduction of nitrite (eq 1), through pathways that are modulated by dioxygen, is an "intelligent" approach, and several organisms, from bacteria to plants and mammals, are using them to generate NO. In humans, these nitrite-dependent pathways are also offering or will create new therapeutic approaches for the management of several pathological conditions, including ischemia injury, cardiovascular dysfunctions, myocardial infarction, stroke, pulmonary hypertension, and even infection.[17−35] As such, the characterization of potential mammalian nitrite reductases is of great interest.

XO/XD and AO, as well as hemoglobin and myoglobin, are some of the most promising mammalian nitrite reductases. In this work, we extended our previous studies of the nitrite reductase activity of mammalian XO and bacterial aldehyde oxidoreductase[43] and characterized nitrite reduction and NO formation by rat and human liver XO/XD and AO. The characterization of the pH profile of the kinetic parameters of XO/XD/AO-catalyzed nitrite reduction (k_{cat}, K_m, and k) and the quantification of dioxygen inhibition demonstrated that it is feasible and reasonable that XO/XD and AO could contribute to *in vivo* NO generation under hypoxic conditions. Cellular NO formation, followed in HepG2 and HMEC, supported the idea that XO/XD and AO can, in fact, contribute to NO generation under hypoxia and even quasi-normoxia inside a living human cell.

ASSOCIATED CONTENT

Supporting Information

Schematic representation of the kinetic mechanism proposed (Scheme S1), from which rate equation S1 was derived, and some pH profiles simulated with this equation (Figure S1). This material is available free of charge via the Internet at http://pubs.acs.org.

AUTHOR INFORMATION

Corresponding Authors

*E-mail: luisa.maia@fct.unl.pt.

*E-mail: jose.moura@fct.unl.pt.

Funding

This work was supported by Projects PTDC/QUI-BIQ/100366/2008 and PEst-C/EQB/LA0006/2013 (Fundação para a Ciência e Tecnologia/MCTES, Portugal).

Notes

The authors declare no competing financial interest.

ACKNOWLEDGMENTS

We are grateful to Mr. João António Vieira and to Instituto de Investigação Científica Bento da Rocha Cabral (Lisbon, Portugal) for the breeding and handling of the Sprague-Dawley rats. We also gratefully acknowledge the collaboration of Dr. Ana Afonso and Dr. Ana Carvalho from Hospital Curry Cabral (Lisbon, Portugal) for providing human liver tissue. In addition, we thank Dr. Luísa Barreira (Universidade do Algarve, Faro, Portugal) and Dr. Carla Afonso (Universidade de Lisboa) for providing the cell lines.

ABBREVIATIONS

AFR, activity-to-flavin ratio; AO, aldehyde oxidase; BMXO, bovine milk XO; CuNiR, bacterial copper-containing nitrite reductase; DAF-FM, 4-amino-5-(methylamino)-2′,7′-difluorofluorescein; DAF-FM DA, DAF-FM diacetate; DHB, dihydroxybenzaldehyde; DMAC, *p*-dimethylaminocinnamaldehyde; DPI, diphenyleneiodonium chloride; EPR, electron paramagnetic resonance; Fe/S, iron−sulfur center; Hb, hemoglobin; HepG2,

DOI: 10.1021/bi500987w
Biochemistry 2015, 54, 685−710

human epithelial cells from liver carcinoma; HL, human liver enzymes; HMEC, human microvascular endothelial cells; MGD, $(MGD)_2$-Fe, and $(MGD)_2$-Fe-NO, *N*-methyl-D-glucamine dithiocarbamate, ferrous complex of MGD, and mononitrosyl–iron complex of MGD; L-NAME, N^{ω}-nitro-L-arginine methyl ester hydrochloride; NiR, nitrite reductase; NO, nitric oxide radical; NOS, NO synthase; NMN, *N*′-methyl-nicotinamide; RL, rat liver enzymes; ROS, reactive oxygen species; SOD, superoxide dismutase; XD, xanthine dehydrogenase; XO, xanthine oxidase.

■ ADDITIONAL NOTES

[a]The rat (*Rattus norvegicus*) genome is characterized by the presence of an aldehyde oxidase gene cluster on chromosome 9q31, which is largely syntenic to mouse chromosome 1 and encodes four enzyme isoforms (AOX1, AOH1, AOH2, and AOH3). We did not attempt to know which hepatic isoform is being purified, but it is likely they are the AOX1 and AOH1 isoforms, as observed in fully developed mice.[79,105−107]

[b]Demolybdo and desulfo forms are enzyme molecules without the molybdenum atom and molecules whose molybdenum atom lacks the equatorial terminal sulfo group, respectively.[58−64] Only XO and AO molecules with an intact Mo=S group (Scheme 1, i) can perform hydroxylation reactions. Therefore, the hydroxylation activity assay constitutes a suitable way to measure the number of XO and AO molecules with the molybdenum center intact. Samples with a larger amount of demolybdo and/or desulfo forms display low hydroxylation activity and, consequently, have lower AFR values.[109,110]

[c]Consider two enzyme-catalyzed reactions that occur separately, "A" with "B" and "A" with "C", for which one can determine the respective individual $K_m^{app,B}$, $k_{cat}^{app,B}$, $K_m^{app,C}$, and $k_{cat}^{app,C}$ values, for a given constant concentration of "A". For a mechanism in which "A" reacts with "B" in the presence of the competitive substrate "C", it can be demonstrated that, in the presence of a constant concentration of "A", (i) the $k_{cat}^{app,B}$ value is the same in the presence and absence of "C" and (ii) the competitive inhibition constant ($K_i^{app,C}$) is equal to the $K_m^{app,C}$ (i.e., is equal to the $K_m^{app,C}$ determined in the absence of "B").[112] In fact, for whatever two reactions, "A" with "B" and "A" with "C", it is better to study the reactions separately, because, in general, the simultaneous presence of competing substrates tends to complicate the analysis, without providing much more information.[112] Although the same demonstration can be done for dioxygen inhibition, the data analysis is more complicated, because several dioxygen-dependent reactions can consume the enzymatically generated NO (described in the text below), thus faking the inhibition.

[d]There are two DAF-FM-based probes, DAF-FM itself and DAF-FM DA. Once the two covalently bound acetate groups of DAF-FM DA are hydrolyzed, both probes are identical.

[e]The molecular mechanism of hydroxylation by both XO and AO has been established on the basis of the XO-catalyzed hydroxylation of xanthine and FYX-051.[58−64,151,152] Nevertheless, the mechanism of aldehyde hydroxylation[60] or another substrate that reacts at the molybdenum site is thought to be essentially the same in both enzymes. The catalysis of hydroxylation[151,152] is initiated by the activation of the molybdenum labile -OH group by the neighboring (conserved) deprotonated glutamate residue, Glu_{1261} (bovine enzyme numbering), to form $Mo^{6+}-O^-$ (base-assisted catalysis) (Scheme 1, ii, a → b), followed by the hydride transfer from substrate (e.g., aldehyde) to the essential Mo=S group, with the simultaneous nucleophilic attack of $Mo-O^-$ on the carbocation formed. This concerted attack results in the formation of a covalent intermediate, $Mo^{4+}-O-C-R$ (−SH) (Scheme 1, ii, c). Subsequently, the product (in the example, carboxylate) is displaced by a water molecule or nitrite (as represented in Scheme 1, ii, c → d).

[f]In spite of the nitrite binding mode in CuNiR being a "bidentate nitrito" mode, it is tempting not to follow all the similarities between the molybdenum- and copper-containing enzymes.

■ REFERENCES

(1) Moncada, S., Palmer, R. M. J., and Higgs, E. A. (1991) Nitric oxide: Physiology, pathophysiology, and pharmacology. *Pharmacol. Rev. 43*, 109−142.

(2) Eiserich, J. P., Patel, R. P., and O'Donnell, V. B. (1998) Pathophysiology of nitric oxide and related species: Free radical reactions and modification of biomolecules. *Mol. Aspects Med. 19*, 221−357.

(3) Pfeiffer, S., Mayer, B., and Hemmens, B. (1999) Nitric oxide: Chemical puzzles posed by a biological messenger. *Angew. Chem., Int. Ed. 38*, 1714−1731.

(4) Stuehr, D. J. (1999) Mammalian nitric oxide synthases. *Biochim. Biophys. Acta 1411*, 217−230.

(5) Alderton, W. K., Cooper, C. E., and Knowles, R. G. (2001) Nitric oxide synthases: Structure, function and inhibition. *Biochem. J. 357*, 593−615.

(6) Beckman, J. S., and Koppenol, W. H. (1996) Nitric oxide, superoxide and peroxynitrite: The good, the bad and the ugly. *Am. J. Physiol. 271*, C1424−C1437.

(7) Feelisch, M., Rassaf, T., Mnaimneh, S., Singh, N., Bryan, N. S., Jourd'Heuil, D., and Kelm, M. (2002) Concomitant S-, N-, and heme-nitros(yl)ation in biological tissues and fluids: Implications for the fate of NO in vivo. *FASEB J. 16*, 1775−1785.

(8) Bryan, N. S., Rassaf, T., Maloney, R. E., Rodriguez, C. M., Saijo, F., Rodriguez, J. R., and Feelisch, M. (2004) Cellular targets and mechanisms of nitros(yl)ation: An insight into their nature and kinetics in vivo. *Proc. Natl. Acad. Sci. U.S.A. 101*, 4308−4313.

(9) Toledo, J. C., Jr., and Augusto, O. (2012) Connecting the chemical and biological properties of nitric oxide. *Chem. Res. Toxicol. 25*, 975−989.

(10) Wink, D. A., Darbyshire, J. F., Nims, R. W., Saavedra, J. E., and Ford, P. C. (1993) Reactions of the bioregulatory agent nitric oxide in oxygenated aqueous media: Determination of the kinetics for oxidation and nitrosation by intermediates generated in the NO/O_2 reaction. *Chem. Res. Toxicol. 6*, 23−27.

(11) Goldstein, S., and Czapski, G. (1995) Kinetics of nitric oxide autoxidation in aqueous solution in the absence and presence of various reductants. The nature of the oxidizing intermediates. *J. Am. Chem. Soc. 117*, 12078−12084.

(12) Shiva, S., Wang, X., Ringwood, L. A., Xu, X., Yuditskaya, S., Annavajjhala, V., Miyajima, H., Hogg, N., Harris, Z. L., and Gladwin, M. T. (2006) Ceruloplasmin is a NO oxidase and nitrite synthase that determines endocrine NO homeostasis. *Nat. Chem. Biol. 2*, 486−493.

(13) Gow, A. J., Luchsinger, B. P., Pawloski, J. R., Singel, D. J., and Stamler, J. S. (1999) The oxyhemoglobin reaction of nitric oxide. *Proc. Natl. Acad. Sci. U.S.A. 96*, 9027−9032.

(14) Flögel, U., Merx, M. W., Gödecke, A., Decking, U. K. M., and Schrader, J. (2001) Myoglobin: A scavenger of bioactive NO. *Proc. Natl. Acad. Sci. U.S.A. 98*, 735−740.

(15) Herold, S., Exner, M., and Nauser, T. (2001) Kinetic and mechanistic studies of the NO-mediated oxidation of oxymyoglobin and oxyhemoglobin. *Biochemistry 40*, 3385−3395.

(16) Joshi, M. S., Ferguson, T. B., Jr., Han, T. H., Hyduke, D. R., Liao, J. C., Rassaf, T., Bryan, N., Feelisch, M., and Lancaster, J. R., Jr. (2002) Nitric oxide is consumed, rather than conserved, by reaction with oxyhemoglobin under physiological conditions. *Proc. Natl. Acad. Sci. U.S.A. 99*, 10341−10346.

DOI: 10.1021/bi500987w
Biochemistry 2015, 54, 685−710

(17) Cosby, K., Partovi, K. S., Crawford, J. H., Patel, R. P., Reiter, C. D., Martyr, S., Yang, B. K., Waclawiw, M. A., Zalos, G., Xu, X., Huang, K. T., Shields, H., Kim-Shapiro, D. B., Schechter, A. N., Cannon, R. O., III, and Gladwin, M. T. (2003) Nitrite reduction to nitric oxide by deoxyhemoglobin vasodilates the human circulation. *Nat. Med. 9*, 1498−1505.
(18) Webb, A., Bond, R., McLean, P., Uppal, R., Benjamin, N., and Ahluwalia, A. (2004) Reduction of nitrite to nitric oxide during ischemia protects against myocardial ischemia-reperfusion damage. *Proc. Natl. Acad. Sci. U.S.A. 101*, 13683−13688.
(19) Duranski, M. R., Greer, J. J., Dejam, A., Jaganmohan, S., Hogg, N., Langston, W., Patel, R. P., Yet, S. F., Wang, X., Kevil, C. G., Gladwin, M. T., and Lefer, D. J. (2005) Cytoprotective effects of nitrite during in vivo ischemia-reperfusion of the heart and liver. *J. Clin. Invest. 115*, 1232−1240.
(20) Lu, P., Liu, F., Yao, Z., Wang, C. Y., Chen, D. D., Tian, Y., Zhang, J. H., and Wu, Y. H. (2005) Nitrite-derived nitric oxide by xanthine oxidoreductase protects the liver against ischemia−reperfusion injury. *Hepatobiliary & Pancreatic Diseases International 4*, 350−355.
(21) Baker, J. E., Su, J., Fu, X., Hsu, A., Gross, G. J., Tweddell, J. S., and Hogg, N. (2007) Nitrite confers protection against myocardial infarction: Role of xanthine oxidoreductase, NADPH oxidase and K(ATP) channels. *J. Mol. Cell. Cardiol. 43*, 437−444.
(22) Dejam, A., Hunter, C. J., Tremonti, C., Pluta, R. M., Hon, Y. Y., Grimes, G., Partovi, K., Pelletier, M. M., Oldfield, E. H., Cannon, R. O., Schechter, A. N., and Gladwin, M. T. (2007) Nitrite infusion in humans and nonhuman primates: Endocrine effects, pharmacokinetics, and tolerance formation. *Circulation 116*, 1821−1831.
(23) Tripatara, P., Patel, N. S., Webb, A., Rathod, K., Lecomte, F. M., Mazzon, E., Cuzzocrea, S., Yaqoob, M. M., Ahluwalia, A., and Thiemermann, C. (2007) Nitrite-derived nitric oxide protects the rat kidney against ischemia/reperfusion injury in vivo: Role for xanthine oxidoreductase. *J. Am. Soc. Nephrol. 18*, 570−580.
(24) Hendgen-Cotta, U. B., Merx, M. W., Shiva, S., Schmitz, J., Becher, S., Klare, J. P., Steinhoff, H., Goedecke, A., Schrader, J., Gladwin, M. T., Kelm, M., and Rassaf, T. (2008) Nitrite reductase activity of myoglobin regulates respiration and cellular viability in myocardial ischemia-reperfusion injury. *Proc. Natl. Acad. Sci. U.S.A. 105*, 10256−10261.
(25) Webb, A. J., Milsom, A. B., Rathod, K. S., Chu, W. L., Qureshi, S., Lovell, M. J., Lecomte, F. M., Perrett, D., Raimondo, C., Khoshbin, E., Ahmed, Z., Uppal, R., Benjamin, N., Hobbs, A. J., and Ahluwalia, A. (2008) Mechanisms underlying erythrocyte and endothelial nitrite reduction to nitric oxide in hypoxia: Role for xanthine oxidoreductase and endothelial nitric oxide synthase. *Circ. Res. 103*, 957−964.
(26) Casey, D. B., Badejo, A. M., Dhaliwal, J. S., Murthy, S. N., Hyman, A. L., Nossaman, B. D., and Kadowitz, P. J. (2009) Pulmonary vasodilator responses to sodium nitrite are mediated by an allopurinol-sensitive mechanism in the rat. *Am. J. Physiol. 296*, H524−H533.
(27) Zuckerbraun, B. S., Shiva, S., Ifedigbo, E., Mathier, M. A., Mollen, K. P., Rao, J., Bauer, P. M., Choi, J. J., Curtis, E., Choi, A. M., and Gladwin, M. T. (2010) Nitrite potently inhibits hypoxic and inflammatory pulmonary arterial hypertension and smooth muscle proliferation via xanthine oxidoreductase-dependent nitric oxide generation. *Circulation 121*, 98−109.
(28) Baliga, R. S., Milsom, A. B., Ghosh, S. M., Trinder, S. L., Macallister, R. J., Ahluwalia, A., and Hobbs, A. J. (2012) Dietary nitrate ameliorates pulmonary hypertension: Cytoprotective role for endothelial nitric oxide synthase and xanthine oxidoreductase. *Circulation 125*, 2922−2932.
(29) Cantu-Medellin, N., and Kelley, E. E. (2013) Xanthine oxidoreductase-catalyzed reduction of nitrite to nitric oxide: Insights regarding where, when and how. *Nitric Oxide 34*, 19−26.
(30) Ghosh, S. M., Kapil, V., Fuentes-Calvo, I., Bubb, K. J., Pearl, V., Milsom, A. B., Khambata, R., Maleki-Toyserkani, S., Yousuf, M., Benjamin, N., Webb, A. J., Caulfield, M. J., Hobbs, A. J., and Ahluwalia, A. (2013) Enhanced vasodilator activity of nitrite in hypertension: Critical role for erythrocytic xanthine oxidoreductase and translational potential. *Hypertension 61*, 1091−1102.
(31) Helms, C., and Kim-Shapiro, D. B. (2013) Hemoglobin-mediated nitric oxide signaling. *Free Radical Biol. Med. 61*, 464−472.
(32) Akrawinthawong, K., Park, J. W., Piknova, B., Sibmooh, N., Fucharoen, S., and Schechter, A. N. (2014) A flow cytometric analysis of the inhibition of platelet reactivity due to nitrite reduction by deoxygenated erythrocytes. *PLoS One 9*, e92435.
(33) Maia, L., and Moura, J. J. G. (2014) How biology handles nitrite. *Chem. Rev. 114*, 5273−5357.
(34) Maia, L., and Moura, J. J. G. (2014) Nitrite reduction by molybdoenzymes: A new class of nitric oxide-forming nitrite reductases. *J. Biol. Inorg. Chem.*, DOI: 10.1007/s00775-014-1234-2.
(35) Omar, S. A., and Webb, A. (2014) Nitrite reduction and cardiovascular protection. *J. Mol. Cell. Cardiol. 73*, 57−69.
(36) Giraldez, R. R., Panda, A., Xia, Y., Sanders, S. P., and Zweier, J. L. (1997) Decreased nitric-oxide synthase activity causes impaired endothelium-dependent relaxation in the postischemic heart. *J. Biol. Chem. 272*, 21420−21426.
(37) Millar, T. M., Stevens, C. R., Benjamin, N., Eisenthal, R., Harrison, R., and Blake, D. R. (1998) Xanthine oxidoreductase catalyses the reduction of nitrates and nitrite to nitric oxide under hypoxic conditions. *FEBS Lett. 427*, 225−228.
(38) Zhang, Z., Naughton, D., Winyard, P. G., Benjamin, N., Blake, D. R., and Symons, M. C. (1998) Generation of nitric oxide by a nitrite reductase activity of xanthine oxidase: A potential pathway for nitric oxide formation in the absence of nitric oxide synthase activity. *Biochem. Biophys. Res. Commun. 249*, 767−772.
(39) Godber, H. L. J., Doel, J. J., Sapkota, G. P., Blake, D. R., Stevens, C. R., Eisenthal, R., and Harrison, R. (2000) Reduction of nitrite to nitric oxide catalyzed by xanthine oxidoreductase. *J. Biol. Chem. 275*, 7757−7763.
(40) Li, H., Samouilov, A., Liu, X., and Zweier, J. L. (2001) Characterization of the magnitude and kinetics of xanthine oxidase-catalyzed nitrite reduction: Evaluation of its role in nitric oxide generation in anoxic tissues. *J. Biol. Chem. 276*, 24482−24489.
(41) Li, H., Samouilov, A., Liu, X., and Zweier, J. L. (2004) Characterization of the effects of oxygen on xanthine oxidase-mediated nitric oxide formation. *J. Biol. Chem. 279*, 16939−16946.
(42) Li, H., Cui, H., Kundu, T. K., Alzawahra, W., and Zweier, J. L. (2008) Nitric oxide production from nitrite occurs primarily in tissues not in the blood: Citical role of xanthine oxidase and aldehyde oxidase. *J. Biol. Chem. 283*, 17855−17863.
(43) Maia, L., and Moura, J. J. G. (2011) Nitrite reduction by xanthine oxidase family enzymes: A new class of nitrite reductases. *JBIC, J. Biol. Inorg. Chem. 16*, 443−460.
(44) Li, H., Kundu, T. K., and Zweier, J. L. (2009) Characterization of the magnitude and mechanism of aldehyde oxidase-mediated nitric oxide production from nitrite. *J. Biol. Chem. 284*, 33850−33858.
(45) Wang, J., Krizowski, S., Fischer, K., Niks, D., Tejero, J., Sparacino-Watkins, C., Wang, L., Ragireddy, P., Frizzell, S., Kelley, E. E., Zhang, Y., Basu, P., Hille, R., Schwarz, G., and Gladwin, M. T. (2014) Sulfite oxidase catalyzes single electron transfer at molybdenum domain to reduce nitrite to nitric oxide. *Antioxid. Redox Signaling*, DOI: 10.1089/ars.2013.5397.
(46) Sparacino-Watkins, C. E., Tejero, J., Sun, B., Gauthier, M. C., Thomas, J., Ragireddy, V., Merchant, B. A., Wang, J., Azarov, I., Basu, P., and Gladwin, M. T. (2014) Nitrite reductase and NO synthase activity of the mitochondrial molybdopterin enzymes mARC1 and mARC2. *J. Biol. Chem. 289*, 10345−10358.
(47) Huang, Z., Shiva, S., Kim-Shapiro, D. B., Patel, R. P., Ringwood, L. A., Irby, C. E., Huang, K. T., Ho, C., Hogg, N., Schechter, A. N., and Gladwin, M. T. (2005) Enzymatic function of hemoglobin as a nitrite reductase that produces NO under allosteric control. *J. Clin. Invest. 115*, 2099−2107.
(48) Gladwin, M. T., and Kim-Shapiro, D. B. (2008) The functional nitrite reductase activity of the heme-globins. *Blood 112*, 2636−2647.
(49) Tiso, M., Tejero, J., Basu, S., Azarov, I., Wang, X., Simplaceanu, V., Frizzell, S., Jayaraman, T., Geary, L., Shapiro, C., Ho, C., Shiva, S., Kim-Shapiro, D. B., and Gladwin, M. T. (2011) Human neuroglobin

DOI: 10.1021/bi500987w
Biochemistry 2015, 54, 685−710

functions as a redox-regulated nitrite reductase. *J. Biol. Chem. 286*, 18277−18289.
(50) Li, H., Hemann, C., Abdelghany, T. M., El-Mahdy, M. A., and Zweier, J. L. (2012) Characterization of the mechanism and magnitude of cytoglobin-mediated nitrite reduction and nitric oxide generation under anaerobic conditions. *J. Biol. Chem. 287*, 36623−36633.
(51) Basu, S., Azarova, N. A., Font, M. D., King, S. B., Hogg, N., Gladwin, M. T., Shiva, S., and Kim-Shapiro, D. B. (2008) Nitrite reductase activity of cytochrome c. *J. Biol. Chem. 283*, 32590−32597.
(52) Li, H., Liu, X., Cui, H., Chen, Y. R., Cardounel, A. J., and Zweier, J. L. (2006) Characterization of the mechanism of cytochrome P450 reductase-cytochrome P450-mediated nitric oxide and nitrosothiol generation from organic nitrates. *J. Biol. Chem. 281*, 12546−12554.
(53) Hendrychova, T., Anzenbacherova, E., Hudecek, J., Skopalik, J., Lange, R., Hildebrandt, P., Otyepka, M., and Anzenbacher, P. (2011) Flexibility of human cytochrome P450 enzymes: Molecular dynamics and spectroscopy reveal important function-related variations. *Biochim. Biophys. Acta 1814*, 58−68.
(54) Castello, P. R., David, P. S., McClure, T., Crook, Z., and Poyton, R. O. (2006) Mitochondrial cytochrome oxidase produces nitric oxide under hypoxic conditions: Implications for oxygen sensing and hypoxic signaling in eukaryotes. *Cell Metab. 3*, 277−287.
(55) Castello, P. R., Woo, D. K., Ball, K., Wojcik, J., Liu, L., and Poyton, R. O. (2008) Oxygen-regulated isoforms of cytochrome c oxidase have differential effects on its nitric oxide production and on hypoxic signaling. *Proc. Natl. Acad. Sci. U.S.A. 105*, 8203−8208.
(56) Aamand, R., Dalsgaard, T., Jensen, F. B., Simonsen, U., Roepstorff, A., and Fago, A. (2009) Generation of nitric oxide from nitrite by carbonic anhydrase: A possible link between metabolic activity and vasodilation. *Am. J. Physiol. 297*, H2068−H2074.
(57) Badejo, A. M., Jr., Hodnette, C., Dhaliwal, J. S., Casey, D. B., Pankey, E., Murthy, S. N., Nossaman, B. D., Hyman, A. L., and Kadowitz, P. (2010) Mitochondrial aldehyde dehydrogenase mediates vasodilator responses of glyceryl trinitrate and sodium nitrite in the pulmonary vascular bed of the rat. *Am. J. Physiol.*, H819−H826.
(58) Hille, R., and Nishino, T. (1995) Xanthine oxidase and xanthine dehydrogenase. *FASEB J. 9*, 995−1003.
(59) Hille, R. (1996) The mononuclear molybdenum enzymes. *Chem. Rev. 96*, 2757−2816.
(60) Hille, R. (2005) Molybdenum-containing hydroxylases. *Arch. Biochem. Biophys. 433*, 107−116.
(61) Hille, R. (2006) Structure and function of xanthine oxidoreductase. *Eur. J. Inorg. Chem.*, 1913−1926.
(62) Nishino, T., Okamoto, K., Eger, B. T., Pai, E. F., and Nishino, T. (2008) Mammalian xanthine oxidoreductase: Mechanism of transition from xanthine dehydrogenase to xanthine oxidase. *FEBS J. 275*, 3278−3289.
(63) Hille, R., Nishino, T., and Bittner, F. (2011) Molybdenum enzymes in higher organisms. *Coord. Chem. Rev. 255*, 1179−1205.
(64) Okamoto, K., Kusano, T., and Nishino, T. (2013) Chemical nature and reaction mechanisms of the molybdenum cofactor of xanthine oxidoreductase. *Curr. Pharm. Des. 19*, 2606−2614.
(65) Della Corte, E., Gozzetti, G., Novello, F., and Stirpe, F. (1969) Properties of the xanthine oxidase from human liver. *Biochim. Biophys. Acta 191*, 164−166.
(66) Parks, D. A., and Granger, D. N. (1986) Xanthine oxidase: Biochemistry, distribution and physiology. *Acta Physiol. Scand., Suppl. 548*, 87−99.
(67) Ichikawa, M., Nishino, T., and Ichikawa, A. (1992) Subcellular localization of xanthine oxidase in rat hepatocytes: High-resolution immunoelectron microscopic study combined with biochemical analysis. *J. Histochem. Cytochem. 40*, 1097−1103.
(68) Sarnesto, A., Linder, N., and Raivio, K. O. (1996) Organ distribution and molecular forms of human xanthine dehydrogenase/xanthine oxidase protein. *Lab. Invest. 74*, 48−56.
(69) Adachi, T., Fukushima, T., Usami, Y., and Hirano, K. (1993) Binding of human xanthine oxidase to sulphated glycosaminoglycans on the endothelial-cell surface. *Biochem. J. 289*, 523−527.
(70) Radi, R., Rubbo, H., Bush, K., and Freeman, B. A. (1997) Xanthine oxidase binding to glycosaminoglycans: Kinetics and superoxide dismutase interactions of immobilized xanthine oxidase−heparin complexes. *Arch. Biochem. Biophys. 339*, 125−135.
(71) Rouquette, M., Page, S., Bryant, R., Benboubetra, M., Stevens, C. R., Blake, D. R., Whish, W. D., Harrison, R., and Tosh, D. (1998) Xanthine oxidoreductase is asymmetrically localised on the outer surface of human endothelial and epithelial cells in culture. *FEBS Lett. 426*, 397−401.
(72) Vickers, S., Schiller, H. J., Hildreth, J. E., and Bulkley, G. B. (1998) Immunoaffinity localization of the enzyme xanthine oxidase on the outside surface of the endothelial cell plasma membrane. *Surgery 124*, 551−560.
(73) Kelley, E. E., Hock, T., Khoo, N. K., Richardson, G. R., Johnson, K. K., Powell, P. C., Giles, G. I., Agarwal, A., Lancaster, J. R., Jr., and Tarpey, M. M. (2006) Moderate hypoxia induces xanthine oxidoreductase activity in arterial endothelial cells. *Free Radical Biol. Med. 40*, 952−959.
(74) Turner, N. A., Doyle, W. A., Ventom, A. M., and Bray, R. C. (1995) Properties of rabbit liver aldehyde oxidase and the relationship of the enzyme to xanthine oxidase and dehydrogenase. *Eur. J. Biochem. 232*, 646−657.
(75) Garattini, E., and Terao, M. (2011) Increasing recognition of the importance of aldehyde oxidase in drug development and discovery. *Drug Metab. Rev. 43*, 374−386.
(76) Enroth, C., Eger, B. T., Okamoto, K., Nishino, T., Nishino, T., and Pai, E. F. (2000) Crystal structures of bovine milk xanthine dehydrogenase and xanthine oxidase: Structure-based mechanism of conversion. *Proc. Natl. Acad. Sci. U.S.A. 97*, 10723−10728.
(77) Ishikita, H., Eger, B. T., Okamoto, K., Nishino, T., and Pai, E. F. (2012) Protein conformational gating of enzymatic activity in xanthine oxidoreductase. *J. Am. Chem. Soc. 134*, 999−1009.
(78) Kooij, A., Schiller, H. J., Schijns, M., Van Noorden, C. J., and Frederiks, W. M. (1994) Conversion of xanthine dehydrogenase into xanthine oxidase in rat liver and plasma at the onset of reperfusion after ischemia. *Hepatology 19*, 1488−1495.
(79) Garattini, E., Fratelli, M., and Terao, M. (2008) Mammalian aldehyde oxidases: Genetics, evolution and biochemistry. *Cell. Mol. Life Sci. 65*, 1019−1048.
(80) Pryde, D. C., Dalvie, D., Hu, Q., Jones, P., Obach, R. S., and Tran, T. D. (2010) Aldehyde oxidase: An enzyme of emerging importance in drug discovery. *J. Med. Chem. 53*, 8441−8460.
(81) Swenson, T. L., and Casida, J. E. (2013) Aldehyde oxidase importance in vivo in xenobiotic metabolism: Imidacloprid nitro-reduction in mice. *Toxicol. Sci. 133*, 22−28.
(82) Landon, E. J., and Myles, M. (1967) NADH oxidation by hypoxanthine dehydrogenase of avian kidney. *Biochim. Biophys. Acta 143*, 429−431.
(83) Massey, V., Brumby, P. E., Komai, H., and Palmer, G. (1969) Studies on milk xanthine oxidase: Some spectral and kinetic properties. *J. Biol. Chem. 244*, 1682−1691.
(84) Mira, L., Maia, L., Barreira, L., and Manso, C. F. (1995) Evidence for free radical generation due to NADH oxidation by aldehyde oxidase during ethanol metabolism. *Arch. Biochem. Biophys. 318*, 53−58.
(85) Maia, L., Vala, A., and Mira, L. (2005) NADH oxidase activity of rat liver xanthine dehydrogenase and xanthine oxidase: Contribution for damage mechanisms. *Free Radical Res. 39*, 979−986.
(86) Maia, L., Duarte, R. O., Ponces-Freire, A., Moura, J. J. G., and Mira, L. (2007) NADH oxidase activity of rat and human liver xanthine oxidoreductase: Potential role in superoxide production. *JBIC, J. Biol. Inorg. Chem. 12*, 777−787.
(87) Kundu, T. K., Velayutham, M., and Zweier, J. L. (2012) Aldehyde oxidase functions as a superoxide generating NADH oxidase: An important redox regulated pathway of cellular oxygen radical formation. *Biochemistry 51*, 2930−2939.
(88) Krenitsky, T. A., Neil, S. M., Elion, G. B., and Hitchings, G. H. (1972) A comparison of the specificities of xanthine oxidase and aldehyde oxidase. *Arch. Biochem. Biophys. 150*, 585−599.

DOI: 10.1021/bi500987w
Biochemistry 2015, 54, 685−710

(89) Hall, W. W., and Krenitsky, T. A. (1986) Aldehyde oxidase from rabbit liver: Specificity toward purines and their analogs. *Arch. Biochem. Biophys. 251*, 36−46.
(90) Li, H., Samouilov, A., Liu, X., and Zweier, J. L. (2003) Characterization of the magnitude and kinetics of xanthine oxidase-catalyzed nitrate reduction: Evaluation of its role in nitrite and nitric oxide generation in anoxic tissues. *Biochemistry 42*, 1150−1159.
(91) Stone, J. R., and Yang, S. (2006) Hydrogen peroxide: A signaling messenger. *Antioxid. Redox Signaling 8*, 243−270.
(92) Veal, E. A., Day, A. M., and Morgan, B. A. (2007) Hydrogen peroxide sensing and signaling. *Mol. Cell 26*, 1−14.
(93) Wright, R. M., and Repine, J. E. (1997) The human molybdenum hydroxylase gene family: Co-conspirators in metabolic free-radical generation and disease. *Biochem. Soc. Trans. 25*, 799−804.
(94) Harrison, R. (2002) Structure and function of xanthine oxidoreductase: Where are we now? *Free Radical Biol. Med. 33*, 774−797.
(95) Stirpe, F., Ravaioli, M., Battelli, M. G., Musiani, S., and Grazi, G. L. (2002) Xanthine oxidoreductase activity in human liver disease. *Am. J. Gastroenterol. 97*, 2079−2085.
(96) Madamanchi, N. R., and Runge, M. S. (2013) Redox signaling in cardiovascular health and disease. *Free Radical Biol. Med. 61*, 473−501.
(97) Granger, D. N., Rutili, G., and McCord, J. M. (1981) Superoxide radicals in feline intestinal ischemia. *Gastroenterology 81*, 22−29.
(98) McCord, J. M. (1985) Oxygen-derived free radicals in postischemic tissue injury. *N. Engl. J. Med. 312*, 159−163.
(99) Zweier, J. L., Kuppusamy, P., and Lutty, G. A. (1988) Measurement of endothelial cell free radical generation: Evidence for a central mechanism of free radical injury in postischemic tissues. *Proc. Natl. Acad. Sci. U.S.A. 85*, 4046−4050.
(100) Nishino, T., Nakanishi, S., Okamoto, K., Mizushima, J., Hori, H., Iwasaki, T., Nishino, T., Ichimori, K., and Nakazawa, H. (1997) Conversion of xanthine dehydrogenase into oxidase and its role in reperfusion injury. *Biochem. Soc. Trans. 25*, 783−786.
(101) Lieber, C. S. (1988) Biochemical and molecular basis of alcohol-induced injury to liver and other tissues. *N. Engl. J. Med. 319*, 1639−1650.
(102) Kato, S., Kawase, T., Alderman, J., Inatomi, N., and Lieber, C. (1990) Role of xanthine oxidase in ethanol-induced lipid peroxidation in rats. *Gastroenterology 98*, 203−210.
(103) Wright, R. M., McManaman, J. L., and Repine, J. E. (1999) Alcohol-induced breast cancer: A proposed mechanism. *Free Radical Biol. Med. 26*, 348−354.
(104) Wu, D., and Cederbaum, A. I. (2003) Alcohol, oxidative stress, and free radical damage. *Alcohol Research & Health 27*, 277−284.
(105) Terao, M., Kurosaki, M., Saltini, G., Demontis, S., Marini, M., Salmona, M., and Garattini, E. (2000) Cloning of the cDNAs coding for two novel molybdo-flavoproteins showing high similarity with aldehyde oxidase and xanthine oxidoreductase. *J. Biol. Chem. 275*, 30690−30700.
(106) Terao, M., Kurosaki, M., Marini, M., Vanoni, M. A., Saltini, G., Bonetto, V., Bastone, A., Federico, C., Saccone, S., Fanelli, R., Salmona, M., and Garattini, E. (2001) Purification of the aldehyde oxidase homolog 1 (AOH1) protein and cloning of the AOH1 and aldehyde oxidase homolog 2 (AOH2) genes: Identification of a novel molybdo-flavoprotein gene cluster on mouse chromosome 1. *J. Biol. Chem. 276*, 46347−46363.
(107) Kurosaki, M., Terao, M., Barzago, M. M., Bastone, A., Bernardinello, D., Salmona, M., and Garattini, E. (2004) The aldehyde oxidase gene cluster in mice and rats: Aldehyde oxidase homologue 3, a novel member of the molybdo-flavoenzyme family with selective expression in the olfactory mucosa. *J. Biol. Chem. 279*, 50482−50498.
(108) Maia, L., and Mira, L. (2002) Xanthine oxidase and aldehyde oxidase: A simple procedure for the simultaneous purification from rat liver. *Arch. Biochem. Biophys. 400*, 48−53.
(109) Saito, T., and Nishino, T. (1989) Differences in redox and kinetic properties between NAD-dependent and O_2-dependent types of rat liver xanthine dehydrogenase. *J. Biol. Chem. 264*, 10015−10022.
(110) Branzoli, U., and Massey, V. (1974) Evidence for an active site persulfide residue in rabbit liver aldehyde oxidase. *J. Biol. Chem. 249*, 4346−4349.
(111) Branzoli, U., and Massey, V. (1974) Preparation of aldehyde oxidase in its native and deflavo forms. *J. Biol. Chem. 249*, 4339−4345.
(112) Cornish-Bowden, A. (1995) *Fundamentals of enzyme kinetics*, Portland Press, London.
(113) Xia, Y., and Zweier, J. L. (1997) Direct measurement of nitric oxide generation from nitric oxide synthase. *Proc. Natl. Acad. Sci. U.S.A. 94*, 12705−12710.
(114) Ichimori, K., Fukahori, M., Nakazawa, H., Okamoto, K., and Nishino, T. (1999) Inhibition of xanthine oxidase and xanthine dehydrogenase by nitric oxide. *J. Biol. Chem. 274*, 7763−7768.
(115) Massey, V., and Edmondson, D. (1970) On the mechanism of inactivation of xanthine oxidase by cyanide. *J. Biol. Chem. 245*, 6595−6598.
(116) Coughlan, M. P., Johnson, J. L., and Rajagopalan, K. V. (1980) Mechanisms of inactivation of molybdoenzymes by cyanide. *J. Biol. Chem. 255*, 2694−2699.
(117) Olson, J. S., Ballou, D. P., Palmer, G., and Massey, V. (1974) The mechanism of action of xanthine oxidase. *J. Biol. Chem. 249*, 4363−4382.
(118) Hunt, J., and Massey, V. (1994) Studies of the reductive half-reaction of milk xanthine dehydrogenase. *J. Biol. Chem. 269*, 18904−18914.
(119) Opie, L. H. (1976) Effects of regional ischemia on metabolism of glucose and fatty acids. Relative rates of aerobic and anaerobic energy production during myocardial infarction and comparison with effects of anoxia. *Circ. Res. 38*, 152−174.
(120) Cobbe, S. M., and Poole-Wilson, P. A. (1980) Tissue acidosis in myocardial hypoxia. *J. Mol. Cell. Cardiol. 12*, 761−770.
(121) Momomura, S., Ingwall, J. S., Parker, J. A., Sahagian, P., Ferguson, J. J., and Grossman, W. (1985) The relationships of high energy phosphates, tissue pH, and regional blood flow to diastolic distensibility in the ischemic dog myocardium. *Circ. Res. 57*, 822−835.
(122) Zweier, J. L., Wang, P., Samouilov, A., and Kuppusamy, P. (1995) Enzyme-independent formation of nitric oxide in biological tissues. *Nat. Med. 1*, 804−809.
(123) Samouilov, A., Kuppusamy, P., and Zweier, J. L. (1998) Evaluation of the magnitude and rate of nitric oxide production from nitrite in biological systems. *Arch. Biochem. Biophys. 357*, 1−7.
(124) Zweier, J. L., Samouilov, A., and Kuppusamy, P. (1999) Non-enzymatic nitric oxide synthesis in biological systems. *Biochim. Biophys. Acta 1411*, 250−262.
(125) Gorenflo, M., Zheng, C., Poge, A., Bettendorf, M., Werle, E., and Fiehn, W. (2001) Metabolites of the L-arginine−NO pathway in patients with left-to-right shunt. *Clin. Lab. 47*, 441−447.
(126) Rodriguez, J., Maloney, R. E., Rassaf, T., Bryan, N. S., and Feelisch, M. (2003) Chemical nature of nitric oxide storage forms in rat vascular tissue. *Proc. Natl. Acad. Sci. U.S.A. 100*, 336−341.
(127) Bryan, N. S., Rassaf, T., Maloney, R. E., Rodriguez, C. M., Saijo, F., Rodriguez, J. J., and Feelisch, M. (2004) Cellular targets and mechanisms of nitros(yl)ation: An insight into their nature and kinetics in vivo. *Proc. Natl. Acad. Sci. U.S.A. 101*, 4308−4313.
(128) Shiva, S., and Gladwin, M. T. (2009) Shining a light on tissue NO stores: Near infrared release of NO from nitrite and nitrosylated hemes. *J. Mol. Cell. Cardiol. 46*, 1−3.
(129) Kim, J. H., Ryan, M. G., Knaut, H., and Hille, R. (1996) The reductive half-reaction of xanthine oxidase: The involvement of prototropic equilibria in the course of the catalytic sequence. *J. Biol. Chem. 271*, 6771−6780.
(130) Xia, M., Dempski, R., and Hille, R. (1999) The reductive half-reaction of xanthine oxidase: Reaction with aldehyde substrates and identification of the catalytically labile oxygen. *J. Biol. Chem. 274*, 3323−3330.
(131) Koppenol, W. H. (1998) The basic chemistry of nitrogen monoxide and peroxynitrite. *Free Radical Biol. Med. 25*, 385−391.
(132) Klug, D., Rabani, J., and Fridovich, I. (1972) A direct demonstration of the catalytic action of superoxide dismutase through the use of pulse radioiysis. *J. Biol. Chem. 247*, 4839−4842.

DOI: 10.1021/bi500987w
Biochemistry 2015, 54, 685−710

(133) Fridovich, I. (1982) Measuring the activity of superoxide dismutases: An embarrassment of riches. In *Superoxide dismuatase* (Oberley, L. W., Ed.) Vol. *1*, pp 69−88, CRC Press, Bora Raton, FL.
(134) Ward, J. P. T. (2008) Oxygen sensors in context. *Biochim. Biophys. Acta 1777*, 1−14.
(135) Williamson, J. R., Steenbergen, C., Rich, T., Deleeuw, G., Barlow, C., and Chance, B. (1977) The nature of ischemic injury in cardiac tissue. In *Pathophysiology and Therapeutics of Myocardial Ischemia*, pp 193−225, Spectrum Publications Inc., New York.
(136) Kobayashi, K., and Neely, J. R. (1983) Effects of ischemia and reperfusion on pyruvate dehydrogenase activity in isolated rat hearts. *J. Mol. Cell. Cardiol. 15*, 359−367.
(137) Williamson, J. R. (1996) Glycolytic control mechanisms. II. Kinetics of intermediate changes during the aerobic-anoxic transitions in perfused rat heart. *J. Biol. Chem. 241*, 5026−5036.
(138) Varadarajan, S. G., Novalija, E., Smart, S. C., and Stowe, D. F. (2001) Changes in $[Na^+]_i$, compartimental $[Ca^{2+}]$, and NADH with dysfunction after global ischemia in intact hearts. *Am. J. Physiol. 280*, H280−H293.
(139) Lartigue-Mattei, C., Chabard, J. L., Bargnoux, H., Petit, J., Berger, J. A., Ristori, J. M., Bussiere, J. L., Catilina, P., and Catilina, M. J. (1990) Plasma and blood assay of xanthine and hypoxanthine by gas chromatography−mass spectrometry: Physiological variations in humans. *J. Chromatogr. 529*, 93−101.
(140) Himmel, H. M., Sadony, V., and Ravens, U. (1991) Quantitation of hypoxanthine in plasma from patients with ischemic heart disease: Adaption of a high-performance liquid chromatographic method. *J. Chromatogr. 568*, 105−115.
(141) Quinlan, G. J., Lamb, N. J., Tilley, R., Evans, T. W., and Gutteridge, J. M. (1997) Plasma hypoxanthine levels in ARDS: Implications for oxidative stress, morbidity, and mortality. *Am. J. Respir. Crit. Care Med. 155*, 479−484.
(142) Pesonen, E. J., Linder, N., Raivio, K. O., Sarnesto, A., Lapatto, R., Hockerstedt, K., Makisalo, H., and Andersson, S. (1998) Circulating xanthine oxidase and neutrophil activation during human liver transplantation. *Gastroenterology 114*, 1009−1015.
(143) Kojima, H., Nakatsubo, N., Kikuchi, K., Kawahara, S., Kirino, Y., Nagoshi, H., Hirata, Y., and Nagano, T. (1998) Detection and imaging of nitric oxide with novel fluorescent indicators: Diaminofluoresceins. *Anal. Chem. 70*, 2446−2453.
(144) Ye, X., Rubakhin, S. S., and Sweedler, J. V. (2008) Detection of nitric oxide in single cells. *Analyst 133*, 423−433.
(145) Treinin, A., and Hayon, E. (1970) Absorption spectra and reaction kinetics of NO_2, N_2O_3, and N_2O_4 in aqueous solution. *J. Am. Chem. Soc. 92*, 5821−5828.
(146) Lee, K. Y., Kuchynka, D. J., and Kochi, J. K. (1990) Redox equilibria of the nitrosonium cation and of its nonbonded complexes. *Inorg. Chem. 29*, 4196−4204.
(147) Ignarro, L. J., Fukuto, J. M., Griscavage, J. M., Rogers, N. E., and Byrns, R. E. (1993) Oxidation of nitric oxide in aqueous solution to nitrite but not nitrate: Comparison with enzymatically formed nitric oxide from L-arginine. *Proc. Natl. Acad. Sci. U.S.A. 90*, 8103−8107.
(148) Grätzel, M., Taniguchi, S., Henglein, and Ber, A. (1970) Pulsradiolytische Untersuchung der NO-Oxydation und des Gleichgewichts $N_2O_3 \rightarrow NO + NO_2$ in wäßriger Lösung. *Ber. Bunsen-Ges. 74*, 488−492.
(149) Ford, P. C., and Lorkovic, I. M. (2002) Mechanistic aspects of the reactions of nitric oxide with transition-metal complexes. *Chem. Rev. 102*, 993−1018.
(150) Roy, S., Khanna, S., Bickerstaff, A. A., Subramanian, S. V., Atalay, M., Bierl, M., Pendyala, S., Levy, D., Sharma, N., Venojarvi, M., Strauch, A., Orosz, C. G., and Sen, C. K. (2003) Oxygen sensing by primary cardiac fibroblasts: A key role of p21(Waf1/Cip1/Sdi1). *Circ. Res. 92*, 264−271.
(151) Okamoto, K., Matsumoto, K., Hille, R., Eger, B. T., Pai, E. F., and Nishino, T. (2004) The crystal structure of xanthine oxidoreductase during catalysis: Implications for reaction mechanism and enzyme inhibition. *Proc. Natl. Acad. Sci. U.S.A. 101*, 7931−7936.
(152) Pauff, J. M., Zhang, J., Bell, C. E., and Hille, R. (2008) Substrate orientation in xanthine oxidase: Crystal structure of enzyme in reaction with 2-hydroxy-6-methylpurine. *J. Biol. Chem. 283*, 4818−4824.
(153) Burgrnayer, S. J. N., and Stlefel, E. I. (1985) Molybdenum enzymes, cofactors, and model systems: The chemical uniqueness of molybdenum. *J. Chem. Educ. 62*, 943−953.
(154) Harlan, E. E., Berg, J. M., and Holm, R. H. (1986) Thermodynamic fitness of molybdenum(IV,VI) complexes for oxygen atom transfer reactions, including those with enzymatic substrates. *J. Am. Chem. Soc. 108*, 6992−7000.
(155) Stiefel, E. I. (1973) Proposed molecular mechanism for the action of molybdenum in enzymes: Coupled proton and electron transfer. *Proc. Natl. Acad. Sci. U.S.A. 70*, 988−992.
(156) Rajapakshe, A., Snyder, R. A., Astashkin, A. V., Bernardson, P., Evans, D. J., Young, C. G., Evans, D. H., and Enemark, J. H. (2009) Insights into the nature of Mo(V) species in solution: Modeling catalytic cycles for molybdenum enzymes. *Inorg. Chim. Acta 362*, 4603−4608.
(157) Ghosh, S., Dey, A., Sun, Y., Scholes, C. P., and Solomon, E. I. (2009) Spectroscopic and computational studies of nitrite reductase: Proton induced electron transfer and backbonding contributions to reactivity. *J. Am. Chem. Soc. 131*, 277−288.
(158) George, G. N., and Bray, R. C. (1988) Studies by electron paramagnetic resonance spectroscopy of xanthine oxidase enriched with molybdenum-95 and with molybdenum-97. *Biochemistry 27*, 3603−3609.
(159) Wilson, G. L., Greenwood, R. J., Pilbrow, J. R., Spence, J. T., and Wedd, A. G. (1991) Molybdenum(V) sites in xanthine oxidase and relevant analogue complexes: Comparison of molybdenum-95 and sulfur-33 hyperfine coupling. *J. Am. Chem. Soc. 113*, 6803−6812.
(160) Doonan, C. J., Rubie, N. D., Peariso, K., Harris, H. H., Knottenbelt, S. Z., George, G. N., Young, C. C., and Kirk, M. L. (2008) Electronic structure description of the cis-MoOS unit in models for molybdenum hydroxylases. *J. Am. Chem. Soc. 130*, 55−65.
(161) Hille, R. (2002) Molybdenum and tungsten in biology. *Trends Biochem. Sci. 27*, 360−367.
(162) Schwarz, G., Mendel, R. R., and Ribbe, M. W. (2009) Molybdenum cofactors, enzymes and pathways. *Nature 460*, 839−847.
(163) Hille, R., and Mendel, R. (2011) Molybdenum in living systems. *Coord. Chem. Rev. 255*, 991−992.
(164) Mendel, R., and Kruse, T. (2012) Cell biology of molybdenum in plants and humans. *Biochim. Biophys. Acta 1823*, 1568−1579.

DOI: 10.1021/bi500987w
Biochemistry 2015, 54, 685−710